


# *In Vivo* Tissue Distribution of Polystyrene or Mixed Polymer Microspheres and Metabolomic Analysis after Oral Exposure in Mice

Marcus M. Garcia,<sup>1</sup> Aaron S. Romero,<sup>2</sup> Seth D. Merkle,<sup>2</sup> Jewel L. Meyer-Hagen,<sup>2</sup> Charles Forbes,<sup>2</sup> Eliane El Hayek,<sup>1</sup> David P. Scieszka,<sup>1</sup> Rachel Templeton,<sup>1,3</sup> Jorge Gonzalez-Estrella,<sup>4</sup> Yan Jin,<sup>5</sup> Haiwei Gu,<sup>5</sup> Angelica Benavidez,<sup>6</sup> Russell P. Hunter,<sup>1</sup> Selita Lucas,<sup>1</sup> Guy Herbert,<sup>1</sup> Kyle Joohyung Kim,<sup>7</sup> Julia Yue Cui,<sup>7</sup> Rama R. Gullapalli,<sup>8</sup> Julie G. In,<sup>2</sup> Matthew J. Campen,<sup>1</sup> and Eliseo F. Castillo<sup>2</sup> 

<sup>1</sup>Department of Pharmaceutical Sciences, College of Pharmacy, University of New Mexico Health Sciences, Albuquerque, New Mexico, USA

<sup>2</sup>Division of Gastroenterology and Hepatology, Department of Internal Medicine, University of New Mexico School of Medicine, Albuquerque, New Mexico, USA

<sup>3</sup>University of Pittsburgh, Pittsburgh, Pennsylvania, USA

<sup>4</sup>School of Civil & Environmental Engineering, Oklahoma State University, Stillwater, Oklahoma, USA

<sup>5</sup>Center for Translational Science, Florida International University, Port St. Lucie, Florida, USA

<sup>6</sup>Center for Micro-Engineered Materials, University of New Mexico, Albuquerque, New Mexico, USA

<sup>7</sup>Department of Environmental & Occupational Health Sciences, University of Washington, Seattle, Washington, USA

<sup>8</sup>Department of Pathology, University of New Mexico Health Sciences, Albuquerque, New Mexico, USA

**BACKGROUND:** Global plastic use has consistently increased over the past century with several different types of plastics now being produced. Much of these plastics end up in oceans or landfills leading to a substantial accumulation of plastics in the environment. Plastic debris slowly degrades into microplastics (MPs) that can ultimately be inhaled or ingested by both animals and humans. A growing body of evidence indicates that MPs can cross the gut barrier and enter into the lymphatic and systemic circulation leading to accumulation in tissues such as the lungs, liver, kidney, and brain. The impacts of mixed MPs exposure on tissue function through metabolism remains largely unexplored.

**OBJECTIVES:** This study aims to investigate the impacts of polymer microspheres on tissue metabolism in mice by assessing the microspheres ability to translocate across the gut barrier and enter into systemic circulation. Specifically, we wanted to examine microsphere accumulation in different organ systems, identify concentration-dependent metabolic changes, and evaluate the effects of mixed microsphere exposures on health outcomes.

**METHODS:** To investigate the impact of ingested microspheres on target metabolic pathways, mice were exposed to either polystyrene (5  $\mu\text{m}$ ) microspheres or a mixture of polymer microspheres consisting of polystyrene (5  $\mu\text{m}$ ), polyethylene (1–4  $\mu\text{m}$ ), and the biodegradability and biocompatible plastic, poly-(lactic-co-glycolic acid) (5  $\mu\text{m}$ ). Exposures were performed twice a week for 4 weeks at a concentration of either 0, 2, or 4 mg/week via oral gastric gavage. Tissues were collected to examine microsphere ingress and changes in metabolites.

**RESULTS:** In mice that ingested microspheres, we detected polystyrene microspheres in distant tissues including the brain, liver, and kidney. Additionally, we report on the metabolic differences that occurred in the colon, liver, and brain, which showed differential responses that were dependent on concentration and type of microsphere exposure.

**DISCUSSION:** This study uses a mouse model to provide critical insight into the potential health implications of the pervasive issue of plastic pollution. These findings demonstrate that orally consumed polystyrene or mixed polymer microspheres can accumulate in tissues such as the brain, liver, and kidney. Furthermore, this study highlights concentration-dependent and polymer type-specific metabolic changes in the colon, liver, and brain after plastic microsphere exposure. These results underline the mobility within and between biological tissues of MPs after exposure and emphasize the importance of understanding their metabolic impact. <https://doi.org/10.1289/EHP13435>

## Introduction

Over the past 50 years, global plastic production has grown exponentially. To date, ~350 million metric tons of plastic are produced globally every year.<sup>1</sup> Much of this plastic ends up in landfills or oceans where it may take several hundred years to degrade depending on composition and environmental factors.<sup>2</sup> Exposure

to light, heat, moisture, and microbes degrades plastic debris into microplastics (MPs), defined as plastic particles smaller than 5 mm.<sup>3</sup> MPs have become ubiquitous throughout our environment, and exposure to humans and animals is thought to occur through ingestion<sup>4–9</sup> or inhalation.<sup>10,11</sup> Multiple studies have reported MP detection in food,<sup>12</sup> salt water,<sup>13</sup> fresh water,<sup>14–16</sup> farming soils,<sup>17</sup> and crops used for both animal and human consumption.<sup>18</sup> A 2019 review of over 50 existing studies on MPs suggests that consumption of common foods and beverages results in humans ingesting ~5 grams of plastic per week.<sup>19</sup> It is currently estimated that by 2050, ~12 billion metric tons of plastic wastes will be released into the environment by bioturbation, atmospheric deposition, sewage irrigation, and landfills,<sup>1,14,17,20</sup> as well as exposure from indoor activities that include the use of laser printers, photocopiers, and three-dimensional (3D) printing as thoroughly reviewed in the following articles.<sup>21–25</sup> With an estimated 3.2 (and growing) metric tons of MPs being released into the environment via commercial and household activities every year, MPs exposure is now unavoidable.<sup>26</sup>

In 2019, the World Health Organization (WHO) released a statement that, based on the limited available evidence, exposure to MPs poses a low concern for human health.<sup>27</sup> However, subsequent reports of cellular and biochemical toxicity of MPs have made it clear that deleterious interactions between MPs and biological systems are concentration-dependent, meaning that the impacts of MPs exposures may increase with time.<sup>28</sup> Ingestion is

---

Address correspondence to Marcus M. Garcia, University of New Mexico Health Sciences, Albuquerque, NM 87131 USA. Email: [marcgarcia@salud.unm.edu](mailto:marcgarcia@salud.unm.edu). And, Matthew J. Campen, University of New Mexico Health Sciences Center, Albuquerque, NM 87131 USA. Email: [mcampen@salud.unm.edu](mailto:mcampen@salud.unm.edu). And, Eliseo F. Castillo, University of New Mexico School of Medicine, Albuquerque, NM 87131 USA. Email: [ecastillo@salud.unm.edu](mailto:ecastillo@salud.unm.edu).

Supplemental Material is available online (<https://doi.org/10.1289/EHP13435>).

The authors declared no potential conflict of interest with respect to the research, authorship, and/or publication of this article.

Conclusions and opinions are those of the individual authors and do not necessarily reflect the policies or views of EHP Publishing or the National Institute of Environmental Health Sciences.

Received 2 June 2023; Revised 5 January 2024; Accepted 23 February 2024; Published 10 April 2024.

**Note to readers with disabilities:** *EHP* strives to ensure that all journal content is accessible to all readers. However, some figures and Supplemental Material published in *EHP* articles may not conform to 508 standards due to the complexity of the information being presented. If you need assistance accessing journal content, please contact [ehpsubmissions@niehs.nih.gov](mailto:ehpsubmissions@niehs.nih.gov). Our staff will work with you to assess and meet your accessibility needs within 3 working days.

believed to be the most common route of MPs exposure.<sup>4–9,29–32</sup> MP exposure in rats,<sup>33</sup> mice,<sup>34,35</sup> and zebrafish<sup>36,37</sup> models has been shown to lead to gut microbiota dysbiosis. Gut dysbiosis is linked to numerous inflammatory and metabolic diseases,<sup>38–43</sup> and studies in zebrafish exposed to MPs have been shown to induce intestinal injury and inflammation.<sup>36,44–48</sup> In contrast to these reports, other studies have concluded MPs caused no intestinal histological damage in the colon of mice.<sup>49,50</sup> In humans, recent evidence show MPs are abundant in colons collected after a colectomy<sup>51</sup> and increased in the stool of individuals with inflammatory bowel disease<sup>52</sup>; however, the effects of MPs on gastrointestinal (GI) health is still being deciphered. Preliminary *in vitro* work has assessed the toxicity and uptake of micro- and nanoplastics in cell lines such as human colorectal adenocarcinoma cells (Caco-2)<sup>53</sup> and human colon intestinal (HT29-MTX-E12)<sup>54</sup> cells as well as a mixture of these cells.<sup>55,56</sup> Additionally, studies in marine animals,<sup>46</sup> rodent organoids,<sup>57</sup> and immune and lung cell cultures<sup>58,59</sup> have shown that MPs can alter cellular energetics and induce oxidative stress and inflammation.

Exposing animals to MPs via the oral gastric route leads to the dissemination of MPs outside of the intestine, specifically the liver.<sup>60</sup> Additionally, several studies in humans, mice, chickens, rats, and zebrafish have shown MP and nanoplastic (NP) ingestion results in their accumulation in tissues such as the placenta,<sup>61</sup> liver,<sup>48,57</sup> and kidney.<sup>62,63</sup> The distribution into the liver caused metabolic changes in mice<sup>30,61</sup> and fish.<sup>34,64,65</sup> These studies highlight how MPs can cross the intestinal barrier and can cause extraintestinal manifestations (e.g., inflammation and oxidative stress). However, there is a lack of evidence regarding the effects of a combination of microplastics. The studies conducted so far have solely focused on investigating the impacts of polystyrene microplastics; they have not examined the metabolic changes that can take place in organs that have a direct interaction with the gut, such as the kidney and brain. As we begin to understand the environmentally relevant sizes, types, and concentrations of MPs humans are ingesting,<sup>9,66–68</sup> researchers are able to further assess the effects of MPs using environmentally relevant concentrations, sizes, and types. The most common MPs include polyethylene (PE), polypropylene (PP), and polystyrene (PS).<sup>69</sup> There are numerous other polymer types that have potential to become microplastics, such as polyester (PES), polyamide (PA), polyurethane (PU), polycarbonate (PC), polyvinyl chloride (PVC), and polyethylene terephthalate (PET) as well as synthetic textiles. Microbeads derived from PE, PP, and PS are commonly used in cosmetics and hygiene products.<sup>70</sup> Other plastics such as poly(lactic-co-glycolic acid) (PLGA) is widely used for microencapsulation and prolonged delivery of materials. PLGA is biodegradable and recognized as being safe by several regulatory agencies in the US and Europe.<sup>71</sup> To date, the systemic impacts of MP ingestion on metabolic pathways in organs have not been studied utilizing environmentally relevant concentrations and mixtures. Given PE and PS are two of the most common MPs that are purposely generated and utilized as microbeads and have leached into the environment,<sup>72</sup> we set out to understand how PS microspheres (5  $\mu\text{m}$ ) and mixed microspheres (1–5  $\mu\text{m}$ ) exposure consisting of PS, PE, and PLGA at environmentally relevant concentrations cross the intestinal barrier and alter metabolism in the colon, liver, and brain. The addition of PLGA was used due to its utilization to encapsulate a broad range of therapeutic agents that delivered via the oral route. Specifically, we evaluated the systemic distribution and metabolic impacts of polystyrene and mixed polymer microsphere ingestion in mice after oral gavage. While not reflective of the myriad environmental MPs, plastic microspheres are a research model that controls for size, shape, and composition, while eliminating the contributions of endotoxin, pyrogens, metals, or other contaminants that may have interactive and confounding effects. Microscopic

visualization and Raman spectroscopy were used to evaluate microsphere accumulation in the colon and translocation to the liver and brain, assess composition postexposure, and identify any physical or chemical changes associated with biological degradation. Targeted and untargeted metabolic profiling was then used to identify functional responses within the colon, liver, and brain. Moreover, we investigated sex-specific effects on the metabolome, conducting analyses with a total of  $n = 4$  males and  $n = 4$  females per exposure group. This study is one of the first to evaluate impacts of not only polystyrene microspheres but also mixed polymer microspheres at an equivalent concentration to what humans are estimated to consume per week.<sup>73</sup>

## Methodology

### Animal Model

Male and female C57BL/6 mice (8–12 wk of age at the beginning of the study) were obtained from Taconic Biosciences (Rensselaer, New York). Animals were housed in an Association for Assessment and Accreditation of Laboratory Animal Care (AAALAC)-approved facility at the University of New Mexico Health Sciences Center. Animals were maintained at constant temperature (20–24°C), relative humidity (30%–60%), and on a 12-h light/dark cycle throughout the study. Animals were provided with normal chow and water *ad libitum*. All experiments were approved by the Institutional Animal Care and Use Committee of the University of New Mexico Health Sciences Center, in accordance with the National Institutes of Health guidelines for use of live animals. The University of New Mexico Health Sciences Center is accredited by the American Association for Accreditation of Laboratory Animal Care.

### Exposure, Tissue Digestion, and Microplastic Isolation

Mice were exposed twice a week to polystyrene or mixed polymer microspheres via oral gastric gavage over a 4-wk period at 0 mg/wk ( $n = 8$ ), 2 mg/wk ( $n = 8$ ), and 4 mg/wk ( $n = 8$ ) of 5  $\mu\text{m}$  microspheres from Degradex (Phosphorex). Exposures were based on an estimated average of between 0.1 and 5 grams of microplastics ingested by humans globally per week through all exposure pathways.<sup>73</sup> Two different microsphere exposures were used for each concentration group; there was a control group (vehicle only) for each type of exposure, for a total of six groups. The two different microsphere exposures were *a*) polystyrene (PS) microspheres (Degradex; catalog number 127) and *b*) a mixed plastics treatment in a 1:1:1 ratio consisting of polystyrene (PS) (Degradex; catalog number 127), polyethylene (PE) (Cospheric; catalog number CPMS-0.96 1–4  $\mu\text{m}$  to 0.2 g), and poly(lactic-co-glycolic acid) (PLGA) (Degradex; catalog number LG5000) microspheres. Prior to gavage, all microspheres were stored based on the manufacturer's recommendations in a 10-mg/ml concentration suspended in deionized water with a small amount of surfactant and 2 mM sodium azide as an antimicrobial agent at 4°C until exposure. Prior to administration, microspheres were washed using vehicle (deionized water). Microspheres were removed in dose concentrations for each gavage of 2 mg or 4 mg per week. These microspheres were centrifuged down at 12,000 $\times g$  for 10 min to remove excess microsphere solution. Then same volume of fresh vehicle was added. Microspheres were vortexed and then respun in centrifuge at 12,000 $\times g$  for 10 min, and washing cycle was repeated for a total of 3 rounds. Each week, the mice were exposed twice weekly at 100  $\mu\text{L}$  per exposure for a total of 2 mg/week or 200  $\mu\text{L}$  per exposure for a total of 4 mg/week. After 4 weeks, the mice were euthanized using isoflurane and exsanguinated, then systemically perfused for one minute and thirty seconds with ice cold saline to

ensure removal of blood from major organs. Serum, brain, liver, kidney, and colon were isolated, snap frozen, and stored at  $-20^{\circ}\text{C}$ . Samples are stored in glass vials to prevent plastic contamination from the postmortem procedures. All mice in each exposure group were housed in polycarbonate cages.

Digestion of the prefrontal cortex of the brain, left lobe of liver, and sagittal cross-section of kidney tissues was performed using  $3\times$  the sample volume of 10% potassium hydroxide (KOH) prepared using deionized water. Samples were incubated at  $40^{\circ}\text{C}$  with agitation for 72 h. Samples were ultracentrifuged (Thermo Scientific Sorvall WX+) at  $30,000\times g$  for 4 h to isolate MPs into a pellet. The supernatant was removed, and the pellet was washed with 100% ethanol (EtOH) and centrifuged at  $15,000\times g$  for 10 min, followed by removal of excess EtOH. The process was repeated three times. After washing, the samples were resuspended in EtOH and stored at  $4^{\circ}\text{C}$  in glass tubes for processing.

To prevent adulteration from airborne and procedural contaminants, we used the following preventative measures: *a*) Latex gloves were worn during all experiments along with 100% cotton lab coats, *b*) all reagents were prepared using ultrapure water (GE LifeSciences; catalog number SH30529.02), *c*) all samples were stored in glass vials (DWK Life Sciences), *d*) all surfaces were covered in absorbent bench coat and cleaned with 70% ETOH prior to experiments, *e*) use of plastic containing equipment was kept to a bare minimum, *f*) and all tools were cleansed and autoclaved prior to use.

### Visualization and Spectroscopic Characterization of Microplastics

**Light microscopy.** Samples of isolated plastics were stored in 100% EtOH in glass tubes for a minimum of 24 h at  $4^{\circ}\text{C}$  before imaging. Slides were prepared by adding 50  $\mu\text{L}$  of sample, and MPs were identified and imaged via polarized light microscopy using an Olympus BX51 microscope. An ultraviolet light source was used to verify that the remaining solids were plastic in nature based on autofluorescence.

**Raman spectroscopy.** Raman Spectroscopy analysis was processed on a WITec Alpha 300R Confocal Raman microscope with a 532-nm laser on isolated microspheres from brain to confirm that microspheres of interest were polystyrene. Additionally, pristine 5- $\mu\text{m}$  polymeric microspheres that underwent 10% potassium hydroxide (KOH) digestion protocol were analyzed to determine if alteration occurred based on biological or chemical degradation. A series of peaks specific to the materials were generated. Substance-specific peaks from an in-house Infrared and Raman Characteristic Group Frequencies library [polystyrene (PS) microspheres (Degradex; catalog number 127); polyethylene (PE) (Cospheric; catalog number CPMS-0.96 1–4  $\mu\text{m}$  to 0.2 g); and poly (lactic-co-glycolic acid) (PLGA) (Degradex; catalog number LG5000) microspheres] were compared to the generated data to identify the materials.

**X-ray photoelectron spectroscopy (XPS) analysis.** A Kratos Ultra DLD spectrometer with a monochromatic Al K $\alpha$  source operating at 150W (1,486.6 eV) was used to perform XPS measurements. The spectrometer was operating at a pressure of  $5\times 10^{-9}$  Torr. Low energy electrons were used to accomplish a charge compensation, and all spectra charges were referenced and adjusted by the C1s region to 285 eV. All high-resolution C1s and survey spectra were acquired at pass energies of 160 and 20 eV and processed using CasaXPS software (version 2.3.25 PR1.0).

### Metabolic Analysis of Colon, Liver, and Brain

Reagents used in this study were all liquid chromatography–mass spectrometry (LC-MS) grade, and all standard components for

measuring metabolites were purchased from both Sigma-Aldrich and Fisher Scientific. Acetonitrile, ammonium acetate, acetic acid, and methanol (MeOH) were purchased from Fisher Scientific. Ammonium hydroxide was purchased from Sigma Aldrich. This study used deionized water that was produced by an in-house water purification system from EMD Millipore (Billerica, MA). Phosphate buffered saline (PBS) was purchased through GE Health care Life Sciences.

### Tissue Preparation

To prepare each tissue sample for analysis,  $\sim 20$  mg of the tissue of interest was homogenized in an Eppendorf tube using a Bullet Blender homogenizer (Next Advance). Each sample was homogenized in 200  $\mu\text{L}$  MeOH:PBS (a 4:1 vol/vol dilution). After completing the initial homogenization, an additional of 800  $\mu\text{L}$  MeOH:PBS was added, and samples were vortexed for 10 s. Thereafter, samples were stored at  $-20^{\circ}\text{C}$  for 30 min, transferred to an ice bath, and sonicated for 30 min. Centrifugation at 14,000 rpm was then performed at  $4^{\circ}\text{C}$  for 10 min, and 800  $\mu\text{L}$  supernatant was transferred to a new Eppendorf tube. Drying of all samples was performed using a CentriVap Concentrator (Labconco) under vacuum, and all residue obtained was reconstituted in 150  $\mu\text{L}$  40% PBS and 60% acetonitrile prior to MS analysis. A portion of all study samples were pooled together to obtain for quality control (QC) samples.

### Targeted Metabolomics

The Agilent 1290 UPLC-6495 QQQ-MS system was utilized to perform liquid chromatography–tandem mass spectrometry (LC-MS/MS) experiments targeting metabolites in the tryptophan metabolic pathway.<sup>74</sup> There were 28 metabolites targeted in this evaluation, including 3-hydroxy anthranilic acid, 3-hydroxykynurenine, 3-indolepropionic acid, 5-hydroxytryptophan, ADP ribose, anthranilic acid, HIAA, indole, indole-3-acetic acid, indole-3-lactic acid, indole-3-pyruvic acid, kynurenic acid, L-kynurenine, melatonin, NAD, NADH, *N'*-formylkynurenine, nicotinamide, nicotinamide mononucleotide, nicotinamide riboside, nicotinic acid, nicotinic acid adenine dinucleotide, nicotinic acid mononucleotide, quinolinic acid, serotonin, tryptamine, tryptophan, and xanthurenic acid. Each sample was injected using a volume of 4  $\mu\text{L}$  and analyzed in positive ionization mode. Chromatographic separations were conducted through a Waters XBridge BEH Amide column in hydrophilic interaction chromatography (HILIC) mode. The flow rate was set to 0.3 mL/min, and the autosampler temperature and column compartment were maintained at  $4^{\circ}\text{C}$  and  $40^{\circ}\text{C}$ , respectively. The mobile phase consisted of two solvents: the first solvent containing 10 mM ammonium acetate and 10 mM ammonium hydroxide in 95% H<sub>2</sub>O and 5% acetonitrile, and the second solvent containing 10 mM ammonium acetate and 10 mM ammonium hydroxide in 95% acetonitrile and 5% H<sub>2</sub>O. An isocratic elution of 90% of the second solvent was performed for 1 min, followed by a decrease to 40% at timepoint  $t = 11$  minutes for 4 min, then gradually increasing back to 90% at timepoint  $t = 15$  minutes. The mass spectrometer was equipped with an electrospray ionization (ESI) source to acquire targeted data in multiple-reaction monitoring (MRM) mode. The LC-MS system employed the Agilent MassHunter workstation software, while the Agilent MassHunter Quantitative Data Analysis Software (version B.07.00) was used to integrate all extracted MRM peaks during analysis. Raw data is found in Excel Tables S3, S4, S7, S8, S11, and S12.

### Untargeted LC-MS Metabolomics

The untargeted LC-MS metabolomics analysis was conducted using a Thermo Scientific Vanquish ultra-high-performance liquid



chromatography (UHPLC) system with a Thermo Scientific Orbitrap Exploris 240 MS (Waltham, MA). Duplicate 1- $\mu$ L samples were analyzed in both negative and positive ionization modes. A Waters XBridge BEH Amide column (150  $\times$  2.1 mm, 2.5- $\mu$ m particle size; Waters Corporation) was used for chromatographic separation in hydrophilic interaction liquid chromatography (HILIC) mode, with a flow rate of 0.3 mL/min, and autosampler temperature was kept at 4°C with the column compartment set to 40°C. The mobile phase A contained 0.1% formic acid in water and the mobile phase B contained 0.1% formic acid in acetonitrile. Other LC conditions including gradients, autosampler, and column temperature were the same as those in targeted metabolomics described above. The mass spectrometer collected untargeted data at 70 to 800  $m/z$  using an electrospray ionization (ESI) source. The spray voltage for the ion source is 3,500 V for positive ionization mode and 3,300 V for negative ionization mode. The Orbitrap resolution for MS1 full scan mode is 120,000. The top 20 scans were selected to trigger in MS2 mode, with resolutions of 60,000 for full scan and 30,000 for data-dependent MS2 (ddMS2), respectively. Additionally, the Higher-energy collisional dissociation (HCD) collision energy mode for MS2 is stepped with a normalized collision energy setting of 30%, 60%, and 150%. MS spectra peaks were identified using  $\sim$  300 aqueous metabolites of in-house chemical standards (Sigma-Aldrich) (Excel Table S13), and compared several commercial MS databases embedded (mzCloud, Predict Composition, Chempider, and Metabolika) in Thermo Scientific Compound Discoverer software 3.3. Limits of 10 ppm for mass accuracy and 100,000 for absolute intensity threshold were set for MS data extraction. Data annotation was based on isotopic pattern, retention time, exact mass, and MS/MS fragmentation patterns. Thermo Scientific Compound Discoverer 3.3 software was used for data processing of aqueous metabolomics data, and peak picking, alignment, and normalization was used for untargeted data. Quality control (QC) pools were established based on the coefficient of variation (CV) <20% and signals showing up in >80% of all samples to ensure high-quality data for analysis.<sup>75</sup> In metabolomics, missing values that exist in more than 20% of samples may be removed from the data, which is called the “80% rule.” Finally, within six groups, the compounds have been identified as follows: brain (1,262 identified, 11,122 unidentified), colon (2,363 identified, 17,312 unidentified), liver (3,042 identified, 19,967 unidentified), Mixed polymer exposed Brain (MB) (2,674 identified, 21,016 unidentified), Mixed polymer exposed Colon (MC) (2,485 identified, 16,047 unidentified), and Mixed polymer exposed Liver (ML) (2,082 identified, 13,983 unidentified). Raw data is found in Excel Tables S1, S2, S5, S6, S9, and S10.

### Statistical Analysis

All samples were analyzed and compared against untreated control mice exposed to vehicle using a  $p = 0.05$  false discovery rate, where appropriate. Pathway analysis and volcano plots were developed using MetaboAnalyst software 5.0 ([www.metaboanalyst.ca](http://www.metaboanalyst.ca)) and validated with Reactome (<https://reactome.org/>)<sup>76,77</sup> (Excel Table S14). Samples were normalized by sum against QC pools. Log transformation was performed, and all data was mean centered.  $p$ -Value threshold was set to 0.05 with equal variance and 2.0-fold change threshold.

## Results

### Visualization of Systemic Microplastic Translocation

To determine whether orally administered microspheres could be translocated from the digestive system, polarized light microscopy was performed on serum, brain, liver, and kidney samples isolated from mice exposed to 0, 2, and 4 mg/week polystyrene and mixed plastic [polystyrene, poly(lactic-co-glycolic acid), and polyethylene]

microspheres for 4 weeks. The presence of polystyrene and mixed polymer microspheres was observed in the serum and in all three isolated tissues (Figure 1 and 2). Although not fully quantifiable with this visualization method, polystyrene and mixed polymer microspheres were readily more apparent in liver samples (Figure 1C) compared with brain and serum, with far fewer polystyrene and mixed polymer microspheres observed in the kidneys. These observations suggest that ingested microspheres may be able to translocate across the gut epithelium into the systemic circulation and accumulate differentially in the assessed organs.

Using Raman spectroscopy and XPS analysis, we wanted to validate that the brain microspheres isolated and viewed under polarized light microscopy were truly polystyrene microspheres. The Raman spectra of the original 5- $\mu$ m polystyrene microspheres were consistent with those particulates found in brain isolates (Figure S1A), and further matched a library polystyrene standard spectra, validating that the systemically translocated and recovered microspheres were polystyrene (Figure 1B2,B3). The microsphere sample recovered from brain isolate, however, did show peak shift differences compared to fresh polystyrene, potentially indicating modification of the surface chemistry or accumulation of other biochemicals (i.e., a corona effect). This observation led us to question whether the alteration was due to the KOH digestion or biological degradation. To address this, we compared the recovered polystyrene microspheres to naïve polystyrene microspheres digested with KOH under the same conditions used in our isolation protocol (Figure S1B). The Raman spectra for the naïve polystyrene microspheres subjected to our isolation protocol was similar to that of the KOH-digested microspheres, suggesting that the KOH digestion did not alter the structure of the polystyrene microspheres.

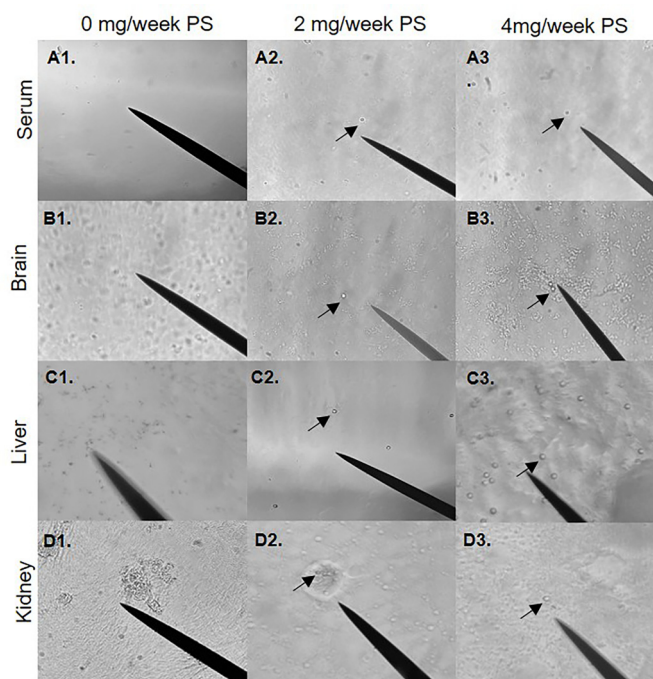


**Figure 1.** Visualization of systemic polystyrene microsphere translocation. Visualization of polystyrene microspheres resuspended from isolated pellet in 100% EtOH. The black arrow indicates polystyrene microspheres. (A1–A3) Five-micrometer polystyrene microspheres in serum (20 $\times$ ). (B1–B3) Five-micrometer polystyrene microspheres in brain (20 $\times$ ). (C1–C3) Five-micrometer polystyrene microspheres in liver (40 $\times$ ). (D1–D3) Five-micrometer polystyrene microspheres in kidney (40 $\times$ ). Mice were exposed twice a week for 4 wk to a low dose of 2 mg/week or a high dose of 4 mg/week with 5- $\mu$ m polystyrene microspheres via oral gavage. Images are representative of  $n = 8$ . Note: EtOH, ethanol.

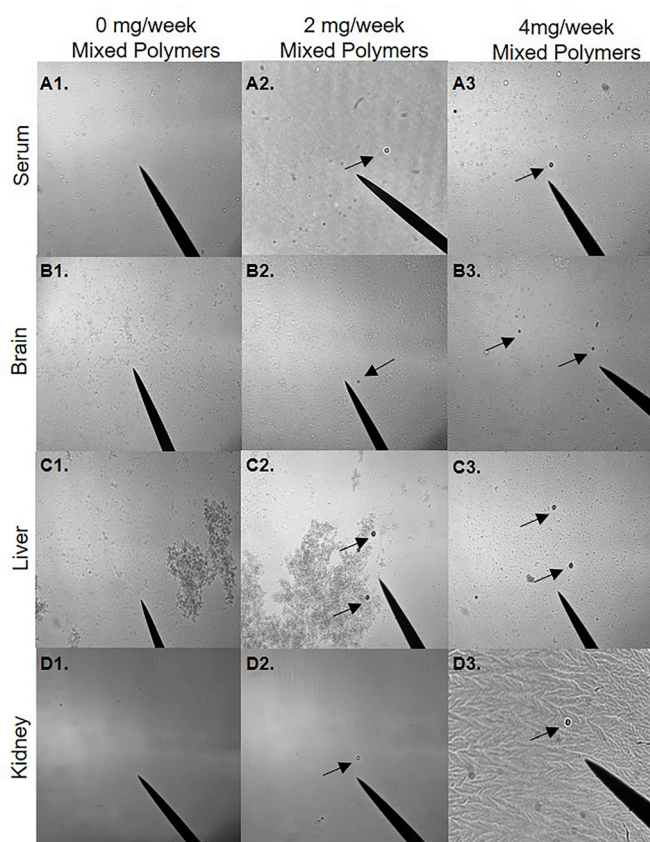


**Figure 2.** Visualization of systemic mixed polymer microsphere translocation. Visualization of mixed polymer microspheres resuspended from isolated pellet in 100% EtOH. The black arrow indicates microspheres. (A1–A3) Five-micrometer mixed polymers [polystyrene (PS), polyethylene (PE), and poly-(lactic-co-glycolic acid) (PLGA)] microspheres in serum (20 $\times$ ). (B1–B3) Five-micrometer mixed polymers (PS, PE, PLGA) in brain (20 $\times$ ). (C1–C3) Five-micrometer mixed polymers (PS, PE, PLGA) in liver (20 $\times$ ). (D1–D3) Five-micrometer mixed polymers (PS, PE, PLGA) in kidney (40 $\times$ ). Mice were exposed twice a week for 4 wk to a low dose of 2 mg/week or a high dose of 4 mg/week with 5- $\mu$ m mixed polymers via oral gavage. Images are representative of  $n = 8$ . Note: EtOH, ethanol.

Given that the liver appeared to have the highest concentrations of microspheres, we wanted to investigate the chemical and surface composition of polystyrene microspheres recovered from the livers of exposed mice compared to naïve polystyrene microspheres using XPS survey scan mode (Figure S1C–E). XPS analysis revealed greater levels of surface potassium and nitrogen in the recovered microspheres, consistent with a biochemical adherence or interaction. XPS analysis also identified fluorine on the surface of the microspheres isolated from liver tissue. We assume that this fluorine peak resulted from the surface adsorption of isoflurane, which was used as a general anesthetic prior to euthanasia in our studies. This fluorine peak may serve as a useful indicator that plastics were obtained from an anesthetized subject, as opposed to derived from *ex vivo* processing or storage of tissue samples in polystyrene containers.

#### Untargeted Metabolic and Pathway Analysis in the Colon

Untargeted metabolomics was performed on colonic tissue metabolites in response to environmentally relevant oral polystyrene and mixed polymer microsphere exposure. Volcano plots for each exposure group showed both significantly higher and lower metabolite levels when compared to control mice (Figure 3A–D). Following the 4-wk exposures, 140 metabolites in the polystyrene-

exposed group and 478 metabolites in the mixed plastics-exposed group were significantly different from control ( $p < 0.05$ ; Figure 3E). We observed that 67 metabolites were uniquely different in the 2-mg/week polystyrene group (Table S1; Excel Table S1) and 53 metabolites were uniquely different in the 4-mg/week polystyrene group (Table S2; Excel Table S2), with 20 (14.3%) significantly different metabolites occurring in both concentration groups (Figure 3E). The mixed plastics exposure groups showed a much higher metabolic response, with 111 uniquely different metabolites in the 2-mg/week exposure group (Table S3; Excel Table S3) and 166 uniquely different metabolites in the 4-mg/week group (Table S4; Excel Table S4). The mixed plastic groups shared 201 (42.0%) metabolites that differed from controls (Figure 3E).

To further understand these changes in metabolites, metabolic pathway analysis was performed. Pathway analysis of metabolite levels in colons from mice exposed to 2 mg/week and 4 mg/week polystyrene compared to controls revealed significant differences from controls ( $p < 0.05$ ) in shared pathways contributing to *a*) biotin metabolism, *b*) histidine metabolism, *c*)  $\beta$ -alanine metabolism, *d*) arginine and proline metabolism, *e*) cytochrome P450 xenobiotic metabolism, and *f*) porphyrin and chlorophyll metabolism (Figure 4A,B). Interestingly, both mixed plastics exposed groups exhibited some overlap in metabolic pathway when compared to the polystyrene only groups including *a*) porphyrin and chlorophyll metabolism, *b*) primary bile acid biosynthesis, *c*) arginine and proline metabolism, *d*) arachidonic acid metabolism, and *e*) the pentose phosphate pathway (Figure 4A–D). Whereas, the 2-mg/week and 4-mg/week mixed plastics groups only shared differences in pathways linked to the *a*) primary bile acid biosynthesis and *b*) the biotin synthesis pathway.

#### Nicotinate and Nicotinamide Metabolic Pathway in the Colon

We also performed targeted metabolic analysis of 28 metabolites associated with nicotinate and nicotinamide metabolic pathway (Figure S2A–D; Table S13). Analysis of colon tissue isolated from mice exposed to polystyrene only revealed one metabolite that was more highly secreted, 5-hydroxytryptophan ( $p = 0.022$ ), in the 2-mg/week exposure group and ( $p = 0.028$ ) in the 4-mg/week exposure group (Table S13). Melatonin ( $p = 0.023$ ) was lower in the 2 mg/week concentration group (Figure S2A,B; Table S13A). The mixed plastics group shared a higher level of kynurenic acid ( $p = 0.004$  in 2 mg/week,  $p = 0.01$  in 4 mg/week), xanthurenic acid ( $p = 0.016$  in 2 mg/week,  $p = 0.027$  in 4 mg/week), melatonin ( $p = 0.037$  in 2 mg/week,  $p = 0.033$  in 4 mg/week), and *N*'-formylkynurenine ( $p = 0.027$  in 2 mg/week,  $p = 0.022$  in 4 mg/week) metabolites (Figure S2C,D; Table S14). A significantly lower level of the nicotinamide ( $p = 0.006$ ) and ADP ribose ( $p = 0.029$ ) metabolites was noted in the 2-mg/week mixed plastic group (Table S14A) while the 4-mg/week mixed plastics group exhibited a significantly lower level of NAD ( $p = 0.042$ ), indole ( $p = 0.027$ ), nicotinic acid ( $p = 0.009$ ), and nicotinic acid adenine dinucleotide ( $p = 0.008$ ) (Table S14B).

#### Oral Gastric Exposure of Plastic Microspheres Effects on Liver Metabolome

Untargeted metabolomics was performed on liver tissues from all microsphere-exposed animals compared to nonexposed mice. Volcano plots for each exposure and concentration group showed patterns of metabolite differences (from control) within each group (Figure 5). We observed that 188 metabolites in the polystyrene-exposed group and 137 metabolites in the mixed plastics-exposed group were significantly different in the plastic microsphere exposure group compared to control ( $p < 0.05$ ). We observed that 129 (68.6%)



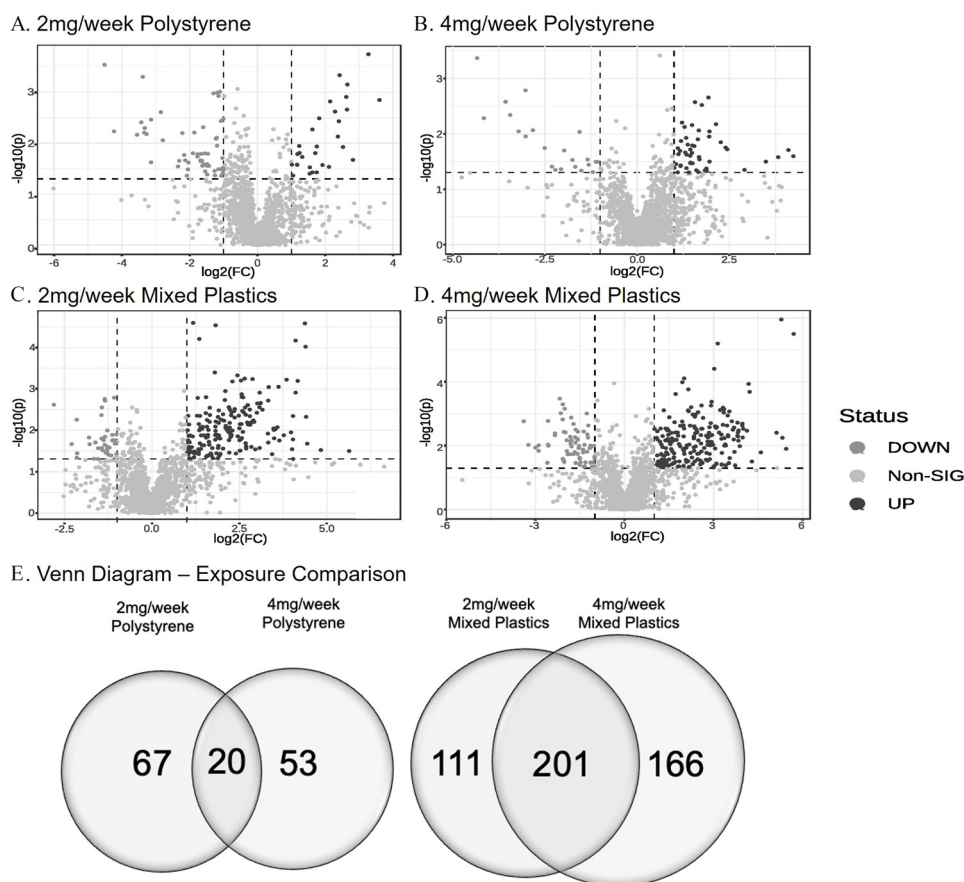


**Figure 3.** Untargeted metabolomics of colon. Untargeted metabolomic analysis in colon tissue of mice exposed to (A) 2 mg/week polystyrene, (B) 4 mg/week polystyrene, (C) 2 mg/week mixed polymer, or (D) 4 mg/week mixed polymer. Data plotted as log(2) fold change ( $p = 0.05$ ). (E) Venn diagram representing the significantly different metabolites following microsphere exposures ( $p < 0.05$  as compared to control). Mice were exposed twice a week for weeks with 5- $\mu\text{m}$  polystyrene microspheres or mixed polymers [polystyrene, polyethylene, and poly-(lactic-co-glycolic acid)] at 2 mg/week (low dose) or 4 mg/week (high dose);  $n = 8$  per group. Source data can be found in Excel Tables S1 and S2.

metabolites were uniquely different in the 2-mg/week polystyrene group (Table S5; Excel Table S5) and 16 (8.5%) metabolites were uniquely different in the 4-mg/week polystyrene group (Table S6; Excel Table S6), with 43 (22.9%) significantly metabolites that were different from control in common between the two different concentrations of PS groups (Figure 5E). In contrast, the mixed plastics exposure groups showed a much higher metabolic response, with 20 (14.6%) uniquely different metabolites in the 2-mg/week exposure group (Table S7; Excel Table S7) and 44 (32.1%) uniquely different metabolites in the 4-mg/week group (Table S8; Excel Table S8), and 73 (53.3%) metabolites that were different from control shared among both mixed polymer concentrations.

To identify the key metabolic pathways altered in the liver following oral microsphere exposure, metabolic pathway analysis was again performed. When comparing the impact on liver metabolic pathways between the 2-mg and 4-mg/week polystyrene-exposed groups, we observed significant differences ( $p < 0.05$ ) in both PS groups in the following pathways: *a*) alanine, aspartate, and glutamate metabolism; *b*) beta-alanine metabolism; *c*) D-glutamine and D-glutamate metabolism; *d*) nitrogen metabolism; *e*) purine metabolism; and *f*) tryptophan metabolism (Figure 6A,B). The beta-alanine and purine metabolic pathways were also altered in the 2-mg/week and 4-mg/week mixed plastic groups, respectively (Figure 6C,D). The 2-mg/week and 4-mg/week mixed plastic groups showed overlap in the *a*) amino acetyl-tRNA biosynthesis pathway, *b*) propanoate metabolism, and *c*) sphingolipid metabolism pathway (Figure 6C,D). The 2-mg/week and 4-mg/week

mixed plastic groups also showed a difference in steroid biosynthesis and steroid metabolism, respectively. Interestingly, among all microsphere-treated groups, there were several pathways associated with amino acids biosynthesis or metabolism that was differentially regulated when compared to untreated mice.

Livers were next examined for metabolites associated with the nicotinate and nicotinamide metabolic pathway via targeted metabolomics. Liver samples from animals exposed to only polystyrene microspheres showed a shared higher expression of nicotinic acid mononucleotide (NMN) and lower expression of 5-hydroxy indoleacetic acid (HIAA) and L-kynurenine in the 2-mg/week exposure and 4-mg/week exposure groups (Figure S3A,B). The mixed plastic-exposed animals showed metabolite differences in both exposure groups; however, the metabolites being significantly higher between these groups were not comparable. In the 2-mg/week mixed plastic exposure group, melatonin was higher and 5-hydroxytryptophan and HIAA were lower (Figure S3C). In contrast, the 4-mg/week mixed plastics exposure group showed a significantly higher expression of metabolites nicotinamide riboside, 3-hydroxykynurenine, nicotinic acid adenine dinucleotide, and NAD and a significantly lower expression of *N'*-formylkynurenine, tryptophan, and indole-3-lactic acid (Figure S3D).

#### Oral Gastric Exposure of PS-Microspheres and Mixed Plastics Effects on Brain Metabolome

To compare PS vs. mixed plastic exposure, the prefrontal cortex of the brain was collected to perform untargeted metabolomics.

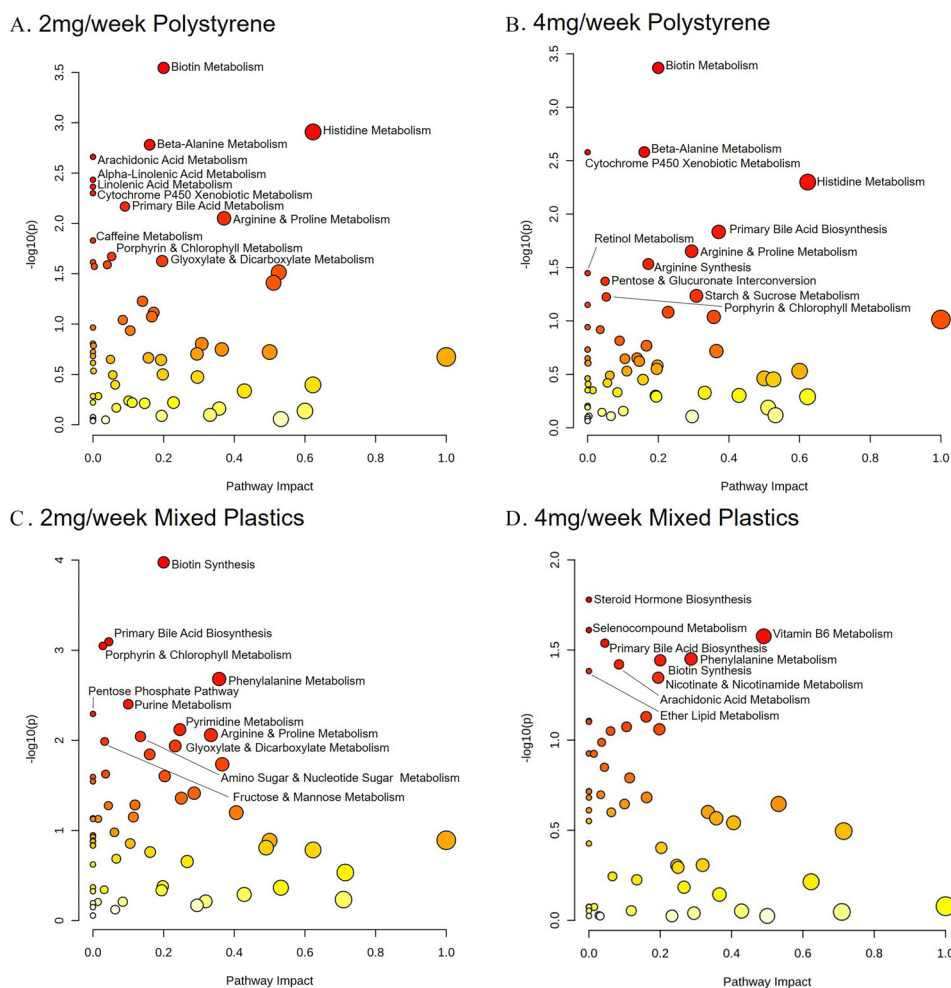


**Figure 4.** Colonic metabolome pathway analysis. Metabolomic pathway analysis of differences in the colon following oral microsphere exposure in mice exposed to (A) 2 mg/week polystyrene, (B) 4 mg/week polystyrene, (C) 2 mg/week mixed polymers, or (D) 4 mg/week mixed polymers. Mice were exposed twice a week for weeks with 5- $\mu$ m polystyrene microspheres or mixed polymers [polystyrene, polyethylene, and poly-(lactic-co-glycolic acid)] at 2 mg/week (low dose) or 4 mg/week (high dose);  $n = 8$  per group. Source data can be found in Excel Tables S1 and S2.

Volcano plots for each exposure group showed patterns of metabolite changes within each group (Figure 7A–D). We observed that 33 metabolites in the polystyrene-exposed group and 50 metabolites in the mixed plastic-exposed group were significantly different due to plastic microsphere exposure ( $p < 0.05$ ). We also observed that 12 (36.4%) metabolites were differently altered in the 2-mg/week polystyrene group (Table S9; Excel Table S9) and 18 (54.5%) metabolites were uniquely different in the 4-mg/week polystyrene group (Table S10; Excel Table S10), with 3 (9.1%) metabolites significantly different from control in both concentration groups (Figure 7E). In contrast, the mixed plastics exposure groups showed a much higher metabolic response, with 3 (6%) uniquely different metabolites in the 2-mg/week group (Table S11; Excel Table S11) and 37 (74%) uniquely different metabolites in the 4-mg/week group (Table S12; Excel Table S12), and 10 (20%) metabolites different from control shared between both of the mixed plastic groups.

To investigate the key metabolic pathways altered by plastic microsphere exposure in the brain, metabolic pathway analysis was again performed. When comparing the brain isolates from 2-mg and 4-mg/week polystyrene-only exposed samples, we observed significant modulation ( $p < 0.05$ ) of the following pathways: *a*) cysteine and methionine metabolism; *b*) glycine, serine, and threonine metabolism; *c*) sphingolipid metabolism; *d*) tyrosine

metabolism; and *e*) the xenobiotic metabolism regulated by cytochrome P450 (Figure 8A,B). Only the xenobiotic metabolism by cytochrome P450 pathway was shared by the 4-mg/week mixed plastic exposure group. Whereas both mixed plastic exposure groups shared a significant modulation in *a*) glycerolipid metabolism and *b*) the steroid biosynthesis pathway (Figure 8C,D). Both the 2-mg/week exposure to PS or mixed polymers displayed alterations in pathways associated with *a*) D-glutamine and D-glutamate metabolism and *b*) nitrogen metabolism. The 4-mg/week exposure to PS or mixed polymers showed significant alterations in pathways associated with the valine, leucine, and isoleucine degradation.

When performing targeted metabolic analysis in the brain for metabolites associated with the nicotinate and nicotinamide metabolic pathway, we found animals exposed to polystyrene only showed higher expression of quinolinic acid and lower of nicotinic acid and tryptamine in the 2-mg/week exposure while the 4-mg/week concentration group did not show any significant differences in expression of metabolites (Figure S4A,B). However, we did see trends of metabolites such as melatonin and nicotinic acid being lower and quinolinic acid and ADP ribose being higher, but these were not always significant. The mixed polymer-exposed group showed multiple metabolite differences in both concentration groups, with NADH being higher

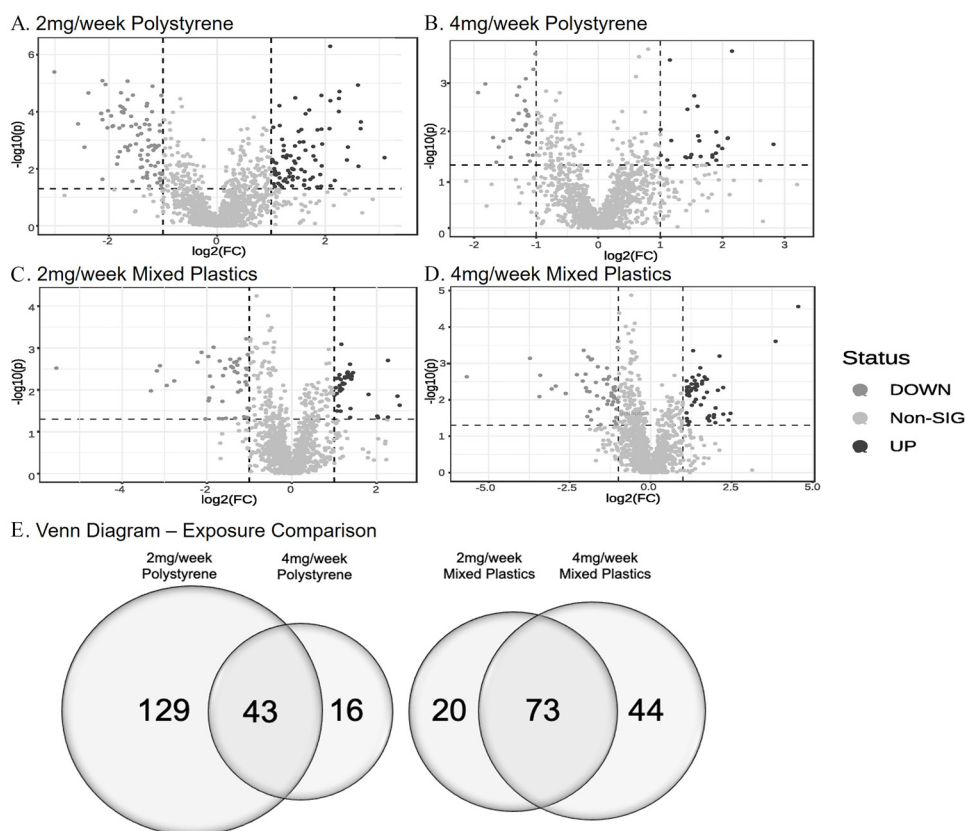


**Figure 5.** Untargeted metabolomics of liver. Untargeted metabolomic analysis in the liver of mice exposed to (A) 2 mg/week polystyrene, (B) 4 mg/week polystyrene, (C) 2 mg/week mixed plastics, or (D) 4 mg/week mixed plastics. Data plotted as  $\log_2$  fold difference ( $p < 0.05$ ). (E) Venn diagram representing the significantly different metabolites following microplastic exposures ( $p < 0.05$  as compared to control). Mice were exposed twice a week for weeks with 5- $\mu\text{m}$  polystyrene microspheres or mixed polymers [polystyrene, polyethylene, and poly-(lactic-co-glycolic acid)] at 2 mg/week (low dose) or 4 mg/week (high dose);  $n = 8$  per group. Source data can be found in Excel Tables S5 and S6.

and L-kynurenine, HIAA, and 3-hydroxykynurenine being significantly lower in both the 2-mg/week and 4-mg/week exposure groups (Figure S4C,D).

## Discussion

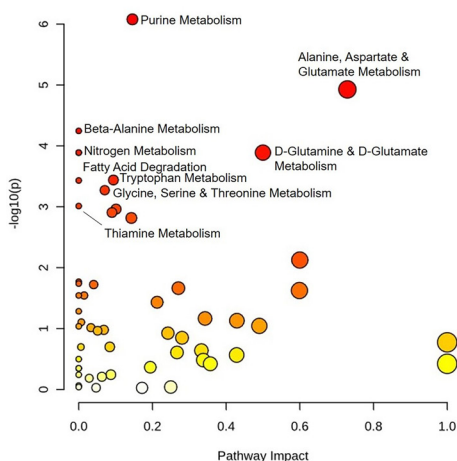
There is no doubt that all living organisms are being exposed to microplastics. While the physiological effects of MP pollution on marine organisms are well-documented,<sup>78–81</sup> the impacts on terrestrial organisms including humans are only beginning to be elucidated. The most common route of exposure appears to be through our diet.<sup>9,80–83</sup> Inhalation intake can also contribute to gut exposure through contaminated mucus ingestion.<sup>84–87</sup> To support this, there have been numerous reports showing in mammals and other species that MPs can accumulate in the gastrointestinal (GI) tract due to their detection in the stool and tissue.<sup>51,52,66,88</sup> Moreover, recent studies showing MP can accumulate in human blood and lungs<sup>10,89,90</sup> suggest that MP can pass the various barriers of the body including the GI tract. Furthermore, this systemic MP accumulation could drastically be increased in individuals with underlying conditions especially those that show signs of increased intestinal permeability such as inflammatory bowel disease (IBD), celiac disease, obesity, and metabolic dysfunction-associated steatotic liver disease (MASLD).<sup>91–96</sup> A few studies have performed both targeted and untargeted metabolomics in the serum,<sup>33,34,60</sup> liver,<sup>97</sup> and stool<sup>66</sup> of micro- and nanoplastic-exposed mice; however, these mice were exposed to a single-type of MP (or NP). Given humans are exposed to a plethora of plastics, we set out to identify, quantify, and compare the colon metabolome of mice

exposed to both concentrations of PS or mixed plastics after a 4-wk exposure.

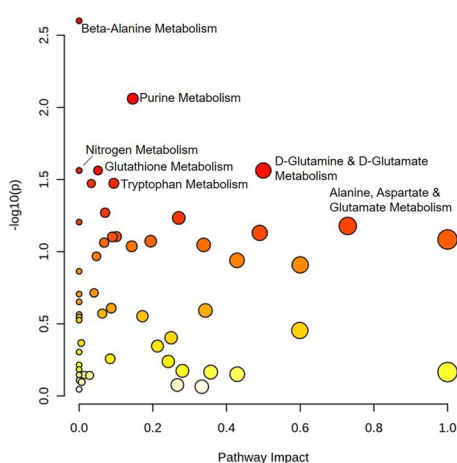
Similar studies have only exposed mice to a single type of MP and then performed metabolomics on either the serum, liver, or stool.<sup>34,60,66,68,97,98</sup> However, humans are being exposed to a plethora of plastics and the assessment of mixed plastic exposure in animal models is critical to understand the true effects of plastic pollution and health outcomes. Our primary focus was on particle uptake, translocation, and impact on biological microenvironments. However, the concern for polymer clearance is an essential aspect to understanding the overall fate and impact of ingested polymers. Clearance mechanisms play a critical role in determining the concentration of these particles within biological tissues. GI issues that need to be considered on this topic include but are not limited to GI motility (contraction and transit), intestinal epithelial absorption, and stool consistency. A limitation of our research is that we did not investigate estimating clearance rates. We do recognize the significance of microplastics being cleared, as microplastics have been found in stool samples from both health and disease-state individuals showing they can be cleared after ingestion.<sup>52,66,99</sup> Nevertheless, our findings provide further support that plastic microspheres can become embedded in other internal organs after ingestion. After oral gastric plastic microsphere exposure in a healthy mouse, we found that microspheres could be detected in distant organs (i.e., brain, liver, and kidney). We hypothesize that the microspheres pass the intestinal epithelial barrier and gut vascular barrier and translocate via the systemic circulation to these organs. Moreover, we show that a four-week PS alone or mixed plastic exposure can impact various metabolic



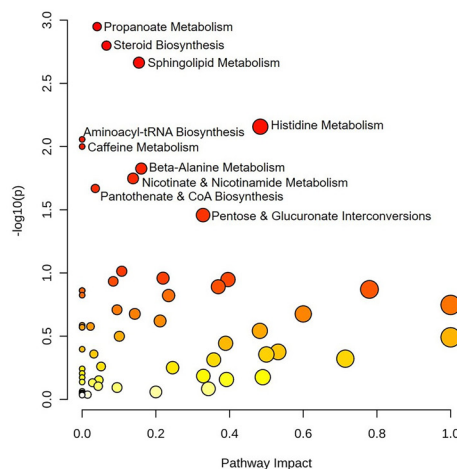
A. 2mg/week Polystyrene



B. 4mg/week Polystyrene



C. 2mg/week Mixed Plastics



D. 4mg/week Mixed Plastics

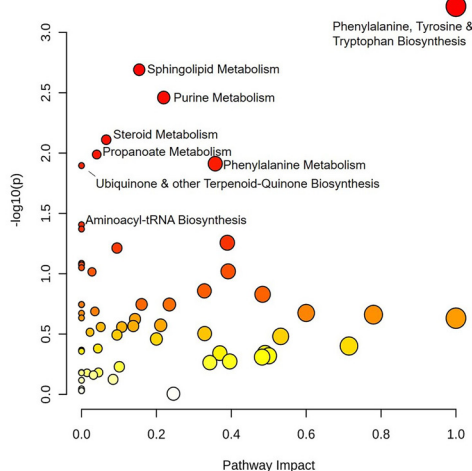


**Figure 6.** Hepatic metabolome pathway analysis. Metabolomic pathway analysis of alterations in the liver following oral MP exposure in mice exposed to (A) 2 mg/week polystyrene, (B) 4 mg/week polystyrene, (C) 2 mg/week mixed polymer, or (D) 4 mg/week mixed polymer. Mice were exposed twice a week for weeks with 5- $\mu$ m polystyrene microspheres or mixed polymers [polystyrene, polyethylene, and poly-(lactic-co-glycolic acid)] at 2 mg/week (low dose) or 4 mg/week (high dose);  $n = 8$  per group. Source data can be found in Excel Tables S5, S6, and S14.

pathways in the colon, liver, and brain of mice when compared to unexposed mice. The colon, liver, and brain showed the most common dysregulated pathways, which showed a link to amino acids. Additionally, we observed differences in metabolic pathways related to purines, pyrimidines, and glutamate, which are products of amino acid metabolism, in our mice exposed to microplastics compared to controls. Amino acids are fundamental for human health as they influence numerous physiological processes, and disruptions in amino acid metabolism have been linked to numerous inflammatory and metabolic diseases.<sup>100–104</sup>

Interestingly, our metabolomics data not only showed differences in the colon, liver, and brain metabolome when comparing our mixed plastic exposure to PS alone groups, but also showed a difference when examining the two concentrations for each group. This became more apparent when we performed targeted metabolomics on the metabolites associated with the nicotinate and nicotinamide metabolic pathway. The greatest impact on the host metabolome was in the following order: colon, liver, and then brain. One reason for these fewer metabolic changes in the brain as compared to the colon and liver may be due to the overall greater apparent accumulation of microspheres in these tissues and the

crosstalk between the gut and liver. Other reasons for more extensive metabolic alterations occurring in the colon and liver may be due to the role that these tissues play in overall break down, digestion, detoxification, and synthesis of consumed products.

In this study, the prefrontal cortex was the only region of the brain evaluated. Thus, we cannot rule out that other portions of the brain may accumulate plastic microspheres and this could cause further changes in the brain metabolome. Additionally, we could not precisely pinpoint the microspheres location due to tissue homogenization. This is a limitation because we acknowledge that the microspheres may be trapped within the vasculature of the brain and have not crossed the blood–brain barrier. Nevertheless, there are still altered metabolic pathways in the brain after polystyrene and mixed polymer microsphere exposure. One alteration of interest was the modulation of the xenobiotic pathway by cytochrome P450 seen in the brain of animals exposed to 4 mg/week of PS and mixed plastics. Although metabolism is primarily carried out in the liver, xenobiotic metabolism by cytochrome P450 alteration in the brain as a result of plastic microsphere exposure could point to potential neurotoxic effects. This data supports the various studies showing that plastic microspheres can be neurotoxic in

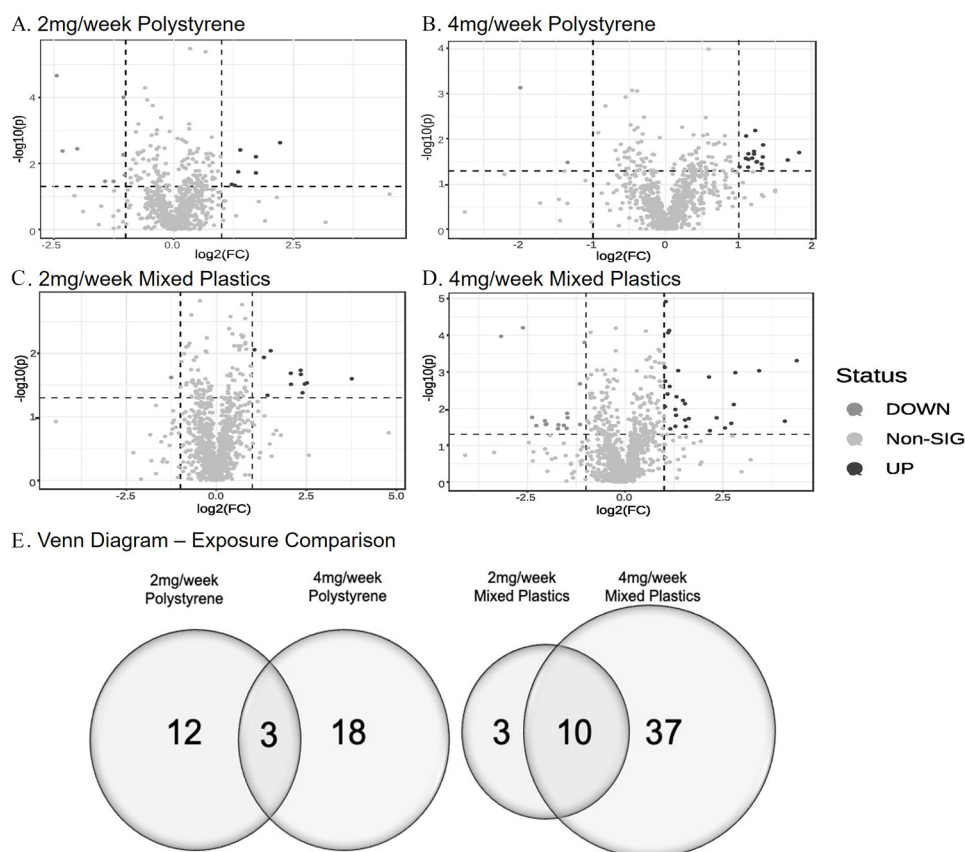


**Figure 7.** Untargeted metabolomics of brain. Untargeted metabolomic analysis of brain isolates from mice exposed to (A) 2 mg/week polystyrene, (B) 4 mg/week polystyrene, (C) 2 mg/week mixed polymer, or (D) 4 mg/week mixed plastics. Data plotted as  $\log_2$  fold change ( $p < 0.05$ ). (E) Venn diagram representing the significantly different metabolites following microplastic exposures ( $p < 0.05$  as compared to control). Mice were exposed twice a week for weeks with 5- $\mu\text{m}$  polystyrene microspheres or mixed polymers [polystyrene, polyethylene, and poly-(lactic-co-glycolic acid)] at 2 mg/week (low dose) or 4 mg/week (high dose);  $n = 8$  per group. Source data can be found in Excel Tables S9 and S10.

mice<sup>105–109</sup> and a more recent paper showing nanoplastics also may affect mouse brain function.<sup>106</sup> A very recent publication has shown microplastics can be detected in the brains of mice after 3 weeks of exposure that ultimately affected behavior.<sup>110</sup> These reports suggest that ingestion of MP/NP over time could cause adverse neurodevelopmental outcomes or trigger the development of neurodegenerative diseases.<sup>111</sup> While this finding requires further investigation, the effects of MPs on our central nervous system may be an interesting avenue for future research.

The results of this study may serve as a model to explore chronic exposure outcomes associated with mixed plastic exposure. Thus, leading to novel techniques to identify their potential risks on human health and future quantitative method development to establish MP-associated metabolite presence. Taken together, our data highlight potential risks that the different types, mixtures, and concentrations of plastic microsphere exposure can impact health outcomes.

### Limitation of Study

Currently, there is substantial research on possible connections of microplastic exposure and poor health outcomes in wildlife, but there has been limited investigation into long-term human health outcomes.<sup>112</sup> When ingested, MPs have the potential to expose organisms to higher concentrations of monomers, polymers, or chemicals associated with the manufacturing process that could potentiate their toxicity.<sup>113</sup> It is believed the micro- and nanoplastics that organisms are ingesting contain chemicals that can further exacerbate plastic-associated toxicity, and this has been reviewed

elsewhere.<sup>114,115</sup> The microplastics utilized in this study were commercially bought and do not contain chemicals such as phthalates, bisphenol A (BPA), or polyfluorinated alkyl substances (PFAs).<sup>116–118</sup> These chemical additives could have an extra layer of problems such as a variety of health effects not limited to altered immune and thyroid function, kidney disease, liver disease, lipid and insulin dysregulation, cancers, and altered reproductive and development outcomes, but we believe our study shows that plastic microsphere exposure can have far-reaching effects after ingestion. Although there is still ongoing research to identify and understand the widespread human health risk of MPs, the current study helped to identify potential organ-specific metabolic pathway alterations that are associated with different types, mixtures, and concentrations of plastic microspheres. Further investigation will need to be performed to identify if these metabolic alterations may play a role in inflammation, immune regulation, metabolism, multiorgan dysfunction, and even potentially exacerbate conditions such as IBD, MASLD, and obesity.<sup>119</sup> Lastly, future studies should focus on novel techniques to adequately identify and quantify microplastics in tissues as well as specific plasticizers. This could help elucidate the functional impacts of altered metabolites due to systemic uptake and distribution of MPs. In pursuit of advancing our study's future direction, we are currently immersed in the development of novel methodology for the quantitation of microplastics within tissue samples. To achieve this, we are employing pyrolysis-gas chromatography–mass spectrometry (Py-GC/MS). This innovative approach promises to provide us with a more comprehensive understanding of the presence and concentration of microplastics

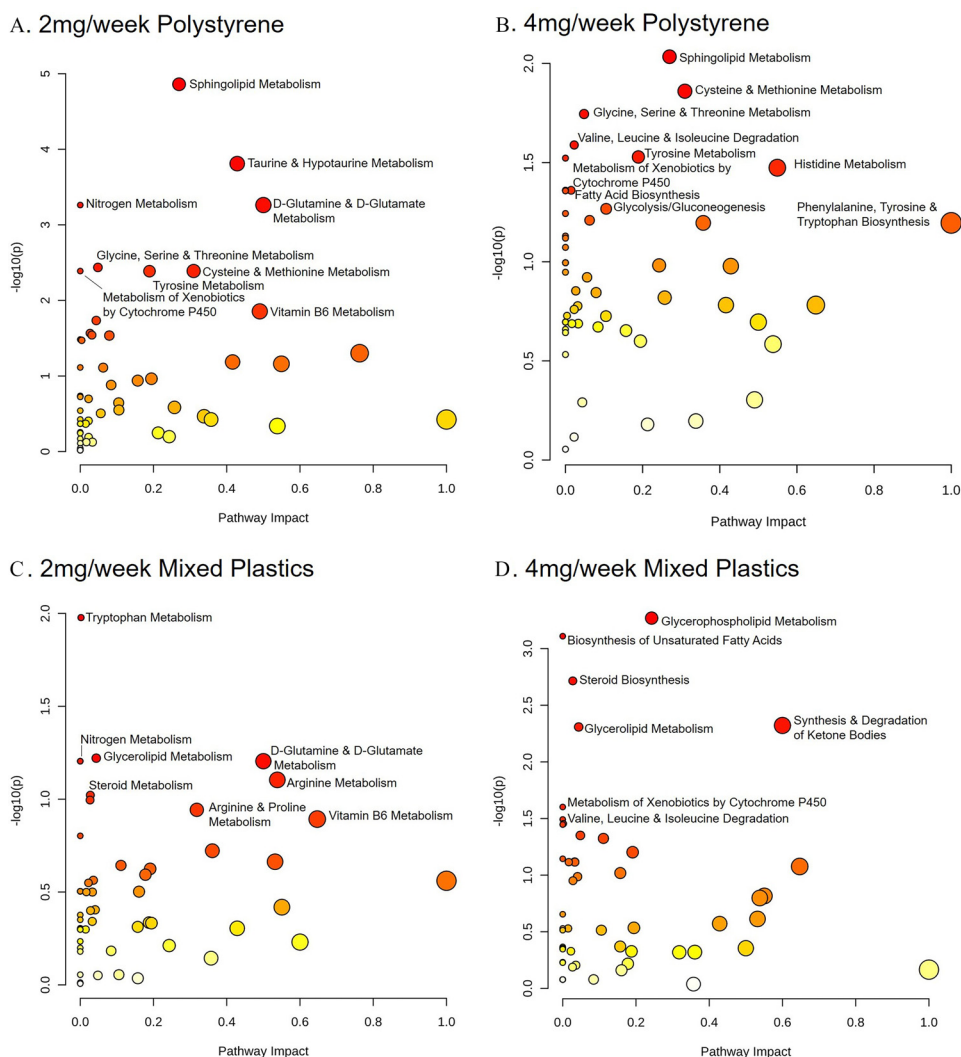


**Figure 8.** Brain metabolome pathway analysis. Metabolomic pathway analysis of alterations in the brain following oral MP exposure in mice exposed to (A) 2 mg/week polystyrene, (B) 4 mg/week polystyrene, (C) 2 mg/week mixed polymer, or (D) 4 mg/week mixed polymer. Mice were exposed twice a week for weeks with 5- $\mu$ m polystyrene microspheres or mixed polymers [polystyrene, polyethylene, and poly-(lactic-co-glycolic acid)] at 2 mg/week (low dose) or 4 mg/week (high dose);  $n = 8$  per group. Source data can be found in Excel Tables S9 and S10.

in biological tissues, thereby significantly contributing to our knowledge of the environmental and health implications associated with these ubiquitous contaminants. We believe Py-GC/MS may help in further identification by quantifying total mass of plastics present. Nevertheless, it is limited in being able to identify particle size, shape, and chemical composition and can be destructive to the sample which will not allow for any other analysis after completion of pyrolysis protocols. The current techniques (e.g., Raman and microscopic visualization) used in this study also have their own limitations. For Raman spectroscopy, while valuable in identifying polymer types, it does have limitations in providing detailed information about size, shape, and surface properties of the particles. Additionally, there is a specific sample size that limits the detection of nanoparticles. Similarly, microscopic visualization is great to visualize the particles but are unable to distinguish between plastic and nonplastic materials. Therefore, new techniques will need to be developed to further characterize and identify microplastics in biological samples.

### Acknowledgments

M.M.G. and A.S.R. performed all analysis, tissue collection, and isolation with the help from S.D.M., J.L.M.H., C.F., E.E.H.,

D.P.S., R.T., J.G.E., A.B., R.P.H., S.L., G.H., K.J.K., J.Y.C., R.R.G., and J.G.I. H.G. and Y.J. contributed to metabolomics and analysis. Exposures were performed by M.M.G., A.S.R., S.L., and G.H. M.M.G., M.J.C., and E.F.C. participated in writing the manuscript. M.M.G., J.G.I., M.J.C., and E.F.C. designed the study, analyzed data, and wrote the paper. All authors approved the final version of the manuscript.

We would like to acknowledge Jesse Benson Hesch for her valuable contribution to the editing of this manuscript. Her expertise and meticulous attention to detail significantly enhanced the quality of our work and preparation of this manuscript.

Funding was supported in part by the National Center for Research Resources and the National Center for Advancing Translational Sciences of the National Institutes of Health (NIH) through NIH grant 1R01 ES032037-01A1 (E.F.C.), in part by UL1TR001449 (E.F.C.), in part by NIH grant P20GM121176 (E.F.C.; J.G.I.) and P20GM130422 (M.J.C.), and in part by NIH grant K12GM088021 (M.M.G.; ASERT-IRACDA), in part by NIMHD grant P50MD015706 (J.G.I.), in part by pilot funding from P20GM130422 (E.E.H.), and in part by P30CA118100.

Studies were conducted with full approval by the Institutional Animal Care and Use Committees of the University of New Mexico.



## References

- Geyer R, Jambeck JR, Law KL. 2017. Production, use, and fate of all plastics ever made. *Sci Adv* 3(7):e1700782, PMID: 28776036, <https://doi.org/10.1126/sciadv.1700782>.
- Bajt O. 2021. From plastics to microplastics and organisms. *FEBS Open Bio* 11(4):954–966, PMID: 33595903, <https://doi.org/10.1002/2211-5463.13120>.
- Anderson PJ, Warrack S, Langen V, Challis JK, Hanson ML, Rennie MD. 2017. Microplastic contamination in Lake Winnipeg, Canada. *Environ Pollut* 225:223–231, PMID: 28376390, <https://doi.org/10.1016/j.envpol.2017.02.072>.
- Pham DT, Kim J, Lee S-H, Kim J, Kim D, Hong S, et al. 2023. Analysis of microplastics in various foods and assessment of aggregate human exposure via food consumption in Korea. *Environ Pollut* 322:121153, PMID: 36709032, <https://doi.org/10.1016/j.envpol.2023.121153>.
- Irnidayanti Y, Soegianto A, Brabo AH, Abdilla FM, Indriyastari KN, Rahmatin NM, et al. 2023. Microplastics in green mussels (*Perna viridis*) from Jakarta Bay, Indonesia, and the associated hazards to human health posed by their consumption. *Environ Monit Assess* 195(7):884, PMID: 37358711, <https://doi.org/10.1007/s10661-023-11535-9>.
- Daniel DB, Ashraf PM, Thomas SN. 2020. Microplastics in the edible and inedible tissues of pelagic fishes sold for human consumption in Kerala, India. *Environ Pollut* 266(pt 2):115365, PMID: 32814179, <https://doi.org/10.1016/j.envpol.2020.115365>.
- Daniel DB, Ashraf PM, Thomas SN, Thomson KT. 2021. Microplastics in the edible tissues of shellfishes sold for human consumption. *Chemosphere* 264(pt 2):128554, PMID: 33049503, <https://doi.org/10.1016/j.chemosphere.2020.128554>.
- Mohsen M, Lin C, Abdalla M, Liu S, Yang H. 2023. Microplastics in canned, salt-dried, and instant sea cucumbers sold for human consumption. *Mar Pollut Bull* 192:115040, PMID: 37216877, <https://doi.org/10.1016/j.marpolbul.2023.115040>.
- Cox KD, Covernton GA, Davies HL, Dower JF, Juanes F, Dudas SE. 2019. Human consumption of microplastics. *Environ Sci Technol* 53(12):7068–7074, PMID: 31184127, <https://doi.org/10.1021/acs.est.9b01517>.
- Amato-Lourenco LF, Oliveira RC, Junior GR, Galvao LDS, Ando RA, Mauad T. 2021. Microplastics inhalation: evidence in human lung tissue. *European Respiratory Journal* 58(suppl 65):PA1792, <https://doi.org/10.1183/13993003.congress-2021.PA1792>.
- Vianello A, Jensen RL, Liu L, Vollertsen J. 2019. Simulating human exposure to indoor airborne microplastics using a breathing thermal manikin. *Sci Rep* 9(1):8670, PMID: 31209244, <https://doi.org/10.1038/s41598-019-45054-w>.
- Udovicki B, Andjelkovic M, Cirkovic-Velickovic T, Rajkovic A. 2022. Microplastics in food: scoping review on health effects, occurrence, and human exposure. *Int J Food Contamination* 9(1):7, <https://doi.org/10.1186/s40550-022-00093-6>.
- Vivekanand AC, Mohapatra S, Tyagi VK. 2021. Microplastics in aquatic environment: challenges and perspectives. *Chemosphere* 282:131151, PMID: 34470176, <https://doi.org/10.1016/j.chemosphere.2021.131151>.
- Ren Z, Gui X, Xu X, Zhao L, Qiu H, Cao X. 2021. Microplastics in the soil-groundwater environment: aging, migration, and co-transport of contaminants – a critical review. *J Hazard Mater* 419:126455, PMID: 34186423, <https://doi.org/10.1016/j.jhazmat.2021.126455>.
- Schymanski D, Oßmann BE, Benismail N, Boukerma K, Dallmann G, von der Esch E, et al. 2021. Analysis of microplastics in drinking water and other clean water samples with micro-Raman and micro-infrared spectroscopy: minimum requirements and best practice guidelines. *Anal Bioanal Chem* 413(24):5969–5994, PMID: 34283280, <https://doi.org/10.1007/s00216-021-03498-y>.
- Schymanski D, Goldbeck C, Humpf HU, Furst P. 2018. Analysis of microplastics in water by micro-Raman spectroscopy: release of plastic particles from different packaging into mineral water. *Water Res* 129:154–162, PMID: 29145085, <https://doi.org/10.1016/j.watres.2017.11.011>.
- Nizzetto L, Futter M, Langaas S. 2016. Are agricultural soils dumps for microplastics of urban origin? *Environ Sci Technol* 50(20):10777–10779, PMID: 27682621, <https://doi.org/10.1021/acs.est.6b04140>.
- Priya AK, Jalil AA, Dutta K, Rajendran S, Vasseghian Y, Qin J, et al. 2022. Microplastics in the environment: recent developments in characteristic, occurrence, identification and ecological risk. *Chemosphere* 298:134161, PMID: 35304213, <https://doi.org/10.1016/j.chemosphere.2022.134161>.
- De Wit W, Biguad N. 2019. *No Plastic in Nature: Assessing Plastic Ingestion From Nature to People*. Geneva, Switzerland: WWF International.
- Rillig MC, Ingraffia R, de Souza Machado AA. 2017. Microplastic incorporation into soil in agroecosystems. *Front Plant Sci* 8:1805, PMID: 29093730, <https://doi.org/10.3389/fpls.2017.01805>.
- Watson-Wright C, Singh D, Demokritou P. 2017. Toxicological implications of released particulate matter during thermal decomposition of nano-enabled thermoplastics. *Nanolmpact* 5:29–40, PMID: 29333505, <https://doi.org/10.1016/j.impact.2016.12.003>.
- Singh D, Schiffman LA, Watson-Wright C, Sotiriou GA, Oyanedel-Craver V, Wohlleben W, et al. 2017. Nanofiller presence enhances polycyclic aromatic hydrocarbon (PAH) profile on nanoparticles released during thermal decomposition of nano-enabled thermoplastics: potential environmental health implications. *Environ Sci Technol* 51(9):5222–5232, PMID: 28397486, <https://doi.org/10.1021/acs.est.6b06448>.
- Pirela SV, Martin J, Bello D, Demokritou P. 2017. Nanoparticle exposures from nano-enabled toner-based printing equipment and human health: state of science and future research needs. *Crit Rev Toxicol* 47(8):683–709, PMID: 28524743, <https://doi.org/10.1080/10408444.2017.1318354>.
- Sotiriou GA, Singh D, Zhang F, Chalbot M-CG, Spielman-Sun E, Hoering L, et al. 2016. Thermal decomposition of nano-enabled thermoplastics: possible environmental health and safety implications. *J Hazard Mater* 305:87–95, PMID: 26642449, <https://doi.org/10.1016/j.jhazmat.2015.11.001>.
- Singh D, Marrocco A, Wohlleben W, Park H-R, Diwadkar AR, Himes BE, et al. 2022. Release of particulate matter from nano-enabled building materials (NEBMs) across their lifecycle: potential occupational health and safety implications. *J Hazard Mater* 422:126771, PMID: 34391975, <https://doi.org/10.1016/j.jhazmat.2021.126771>.
- Boucher J, Friot D. 2017. *Primary Microplastics in the Oceans: A Global Evaluation of Sources*. Gland, Switzerland: International Union for Conservation of Nature.
- WHO (World Health Organization). 2019. *WHO Calls for More Research into Microplastics and Crackdown on Plastic Pollution*. Geneva, Switzerland: WHO.
- Hirt N, Body-Malapel M. 2020. Immunotoxicity and intestinal effects of nano- and microplastics: a review of the literature. *Part Fibre Toxicol* 17(1):57, PMID: 33183327, <https://doi.org/10.1186/s12989-020-00387-7>.
- Montero V, Chinchilla Y, Gómez L, Flores A, Medaglia A, Guillén R, et al. 2023. Human health risk assessment for consumption of microplastics and plasticizing substances through marine species. *Environ Res* 237(pt 1):116843, PMID: 37558111, <https://doi.org/10.1016/j.envres.2023.116843>.
- Shruti VC, Perez-Guevara F, Kutralam-Muniasamy G. 2020. Metro station free drinking water fountain- a potential “microplastics hotspot” for human consumption. *Environ Pollut* 261:114227, PMID: 32113111, <https://doi.org/10.1016/j.envpol.2020.114227>.
- Van Cauwenberghle L, Janssen CR. 2014. Microplastics in bivalves cultured for human consumption. *Environ Pollut* 193:65–70, PMID: 25005888, <https://doi.org/10.1016/j.envpol.2014.06.010>.
- Ziino G, Nalbone L, Giarratana F, Romano B, Cincotta F, Panebianco A. 2021. Microplastics in vacuum packages of frozen and glazed icefish (*Neosalanx* spp.): a freshwater fish intended for human consumption. *Ital J Food Saf* 10(4):9974, PMID: 35071060, <https://doi.org/10.4081/ijfs.2021.9974>.
- Zhao N, Zhao M, Jin H. 2023. Microplastic-induced gut microbiota and serum metabolic disruption in Sprague-Dawley rats. *Environ Pollut* 320:121071, PMID: 36646405, <https://doi.org/10.1016/j.envpol.2023.121071>.
- Jin Y, Lu L, Tu W, Luo T, Fu Z. 2019. Impacts of polystyrene microplastic on the gut barrier, microbiota and metabolism of mice. *Sci Total Environ* 649:308–317, PMID: 30176444, <https://doi.org/10.1016/j.scitotenv.2018.08.353>.
- Lu L, Wan Z, Luo T, Fu Z, Jin Y. 2018. Polystyrene microplastics induce gut microbiota dysbiosis and hepatic lipid metabolism disorder in mice. *Sci Total Environ* 631–632:449–458, PMID: 29529433, <https://doi.org/10.1016/j.scitotenv.2018.03.051>.
- Jin Y, Xia J, Pan Z, Yang J, Wang W, Fu Z. 2018. Polystyrene microplastics induce microbiota dysbiosis and inflammation in the gut of adult zebrafish. *Environ Pollut* 235:322–329, PMID: 29304465, <https://doi.org/10.1016/j.envpol.2017.12.088>.
- Zhao Y, Qin Z, Huang Z, Bao Z, Luo T, Jin Y. 2021. Effects of polyethylene microplastics on the microbiome and metabolism in larval zebrafish. *Environ Pollut* 282:117039, PMID: 33838439, <https://doi.org/10.1016/j.envpol.2021.117039>.
- Sata Y, Marques FZ, Kaye DM. 2020. The emerging role of gut dysbiosis in cardio-metabolic risk factors for heart failure. *Curr Hypertens Rep* 22(5):38, PMID: 32385705, <https://doi.org/10.1007/s11906-020-01046-0>.
- Aron-Wisnewsky J, Prifti E, Belda E, Ichou F, Kayser BD, Dao MC, et al. 2019. Major microbiota dysbiosis in severe obesity: fate after bariatric surgery. *Gut* 68(1):70–82, PMID: 29899081, <https://doi.org/10.1136/gutjnl-2018-316103>.
- Boursier J, Mueller O, Barret M, Machado M, Fizanne L, Araujo-Perez F, et al. 2016. The severity of nonalcoholic fatty liver disease is associated with gut dysbiosis and shift in the metabolic function of the gut microbiota. *Hepatology* 63(3):764–775, PMID: 26600078, <https://doi.org/10.1002/hep.28356>.
- Kaur N, Chen CC, Luther J, Kao JY. 2011. Intestinal dysbiosis in inflammatory bowel disease. *Gut Microbes* 2(4):211–216, PMID: 21983063, <https://doi.org/10.4161/gmic.2.4.17863>.
- Joossens M, Huys G, Cnockaert M, De Preter V, Verbeke K, Rutgeerts P, et al. 2011. Dysbiosis of the faecal microbiota in patients with Crohn’s disease and their unaffected relatives. *Gut* 60(5):631–637, PMID: 21209126, <https://doi.org/10.1136/gut.2010.223263>.
- Tamboli CP, Neut C, Desreumaux P, Colombel JF. 2004. Dysbiosis in inflammatory bowel disease. *Gut* 53(1):1–4, PMID: 14684564, <https://doi.org/10.1136/gut.53.1.1>.
- Limonta G, Mancia A, Benkhalqui A, Bertolucci C, Abelli L, Fossi MC, et al. 2019. Microplastics induce transcriptional changes, immune response and

- behavioral alterations in adult zebrafish. *Sci Rep* 9(1):15775, PMID: 31673028, <https://doi.org/10.1038/s41598-019-52292-5>.
45. Qiao R, Deng Y, Zhang S, Wolosker MB, Zhu Q, Ren H, et al. 2019. Accumulation of different shapes of microplastics initiates intestinal injury and gut microbiota dysbiosis in the gut of zebrafish. *Chemosphere* 236:124334, PMID: 31310986, <https://doi.org/10.1016/j.chemosphere.2019.07.065>.
  46. Qiao R, Sheng C, Lu Y, Zhang Y, Ren H, Lemos B. 2019. Microplastics induce intestinal inflammation, oxidative stress, and disorders of metabolome and microbiome in zebrafish. *Sci Total Environ* 662:246–253, PMID: 30690359, <https://doi.org/10.1016/j.scitotenv.2019.01.245>.
  47. Wan Z, Wang C, Zhou J, Shen M, Wang X, Fu Z, et al. 2019. Effects of polystyrene microplastics on the composition of the microbiome and metabolism in larval zebrafish. *Chemosphere* 217:646–658, PMID: 30448747, <https://doi.org/10.1016/j.chemosphere.2018.11.070>.
  48. Lu Y, Zhang Y, Deng Y, Jiang W, Zhao Y, Geng J, et al. 2016. Uptake and accumulation of polystyrene microplastics in zebrafish (*Danio rerio*) and toxic effects in liver. *Environ Sci Technol* 50(7):4054–4060, PMID: 26950772, <https://doi.org/10.1021/acs.est.6b00183>.
  49. Stock V, Böhmert L, Lisicki E, Block R, Cara-Carmona J, Pack LK, et al. 2019. Uptake and effects of orally ingested polystyrene microplastic particles in vitro and in vivo. *Arch Toxicol* 93(7):1817–1833, PMID: 31139862, <https://doi.org/10.1007/s00204-019-02478-7>.
  50. Sun H, Chen N, Yang X, Xia Y, Wu D. 2021. Effects induced by polyethylene microplastics oral exposure on colon mucin release, inflammation, gut microflora composition and metabolism in mice. *Ecotoxicol Environ Saf* 220:112340, PMID: 34015635, <https://doi.org/10.1016/j.ecoenv.2021.112340>.
  51. Ibrahim YS, Tuan Anuar S, Azmi AA, Wan Mohd Khalik WMA, Lehata S, Hamzah SR, et al. 2021. Detection of microplastics in human colectomy specimens. *JGH Open* 5(1):116–121, PMID: 33490620, <https://doi.org/10.1002/jgh3.12457>.
  52. Yan Z, Liu Y, Zhang T, Zhang F, Ren H, Zhang Y. 2022. Analysis of microplastics in human feces reveals a correlation between fecal microplastics and inflammatory bowel disease status. *Environ Sci Technol* 56(1):414–421, PMID: 34935363, <https://doi.org/10.1021/acs.est.1c03924>.
  53. Wu B, Wu X, Liu S, Wang Z, Chen L. 2019. Size-dependent effects of polystyrene microplastics on cytotoxicity and efflux pump inhibition in human caco-2 cells. *Chemosphere* 221:333–341, PMID: 30641374, <https://doi.org/10.1016/j.chemosphere.2019.01.056>.
  54. Herrala M, Huovinen M, Järvelä E, Hellman J, Tolonen P, Lahtela-Kakkonen M, et al. 2023. Micro-sized polyethylene particles affect cell viability and oxidative stress responses in human colorectal adenocarcinoma Caco-2 and HT-29 cells. *Sci Total Environ* 867:161512, PMID: 36626990, <https://doi.org/10.1016/j.scitotenv.2023.161512>.
  55. DeLoid GM, Cao X, Bitounis D, Singh D, Llopis PM, Buckley B, et al. 2021. Toxicity, uptake, and nuclear translocation of ingested micro-nanoplastics in an in vitro model of the small intestinal epithelium. *Food Chem Toxicol* 158:112609, PMID: 34673181, <https://doi.org/10.1016/j.fct.2021.112609>.
  56. DeLoid GM, Cao X, Coreaas R, Bitounis D, Singh D, Zhong W, et al. 2022. Incineration-generated polyethylene micro-nanoplastics increase triglyceride lipolysis and absorption in an in vitro small intestinal epithelium model. *Environ Sci Technol* 56(17):12288–12297, PMID: 35973094, <https://doi.org/10.1021/acs.est.2c03195>.
  57. Cheng W, Li X, Zhou Y, Yu H, Xie Y, Guo H, et al. 2022. Polystyrene microplastics induce hepatotoxicity and disrupt lipid metabolism in the liver organoids. *Sci Total Environ* 806(pt 1):150328, PMID: 34571217, <https://doi.org/10.1016/j.scitotenv.2021.150328>.
  58. Merkley SD, Moss HC, Goodfellow SM, Ling CL, Meyer-Hagen JL, Weaver J, et al. 2022. Polystyrene microplastics induce an immunometabolic active state in macrophages. *Cell Biol Toxicol* 38(1):31–41, PMID: 34021430, <https://doi.org/10.1007/s10565-021-09616-x>.
  59. El Hayek E, Castillo E, In JG, Garcia M, Cerrato J, Brearley A, et al. 2023. Photoaging of polystyrene microspheres causes oxidative alterations to surface physicochemistry and enhances airway epithelial toxicity. *Toxicol Sci* 193(1):90–102, PMID: 36881996, <https://doi.org/10.1093/toxsci/kfad023>.
  60. Deng Y, Zhang Y, Lemos B, Ren H. 2017. Tissue accumulation of microplastics in mice and biomarker responses suggest widespread health risks of exposure. *Sci Rep* 7:46687, PMID: 28436478, <https://doi.org/10.1038/srep46687>.
  61. Cary CM, DeLoid GM, Yang Z, Bitounis D, Polunas M, Goedken MJ, et al. 2023. Ingested polystyrene nanospheres translocate to placenta and fetal tissues in pregnant rats: potential health implications. *Nanomaterials* (Basel) 13(4):720, PMID: 36839088, <https://doi.org/10.3390/nano13040720>.
  62. Xiong X, Gao L, Chen C, Zhu K, Luo P, Li L. 2023. The microplastics exposure induce the kidney injury in mice revealed by RNA-seq. *Ecotoxicol Environ Saf* 256:114821, PMID: 36989554, <https://doi.org/10.1016/j.ecoenv.2023.114821>.
  63. Meng X, Yin K, Zhang Y, Wang D, Lu H, Hou L, et al. 2022. Polystyrene microplastics induced oxidative stress, inflammation and necroptosis via NF-kappaB and RIP1/RIP3/MLKL pathway in chicken kidney. *Toxicology* 478:153296, PMID: 36029908, <https://doi.org/10.1016/j.tox.2022.153296>.
  64. Cheung LTO, Lui CY, Fok L. 2018. Microplastic contamination of wild and captive flathead grey mullet (*Mugil cephalus*). *Int J Environ Res Public Health* 15(4):597, PMID: 29587444, <https://doi.org/10.3390/ijerph15040597>.
  65. Jing J, Zhang L, Han L, Wang J, Zhang W, Liu Z, et al. 2022. Polystyrene micro-/nanoplastics induced hematopoietic damages via the crosstalk of gut microbiota, metabolites, and cytokines. *Environ Int* 161:107131, PMID: 35149446, <https://doi.org/10.1016/j.envint.2022.107131>.
  66. Schwabl P, Köppel S, Königshofer P, Bucsecs T, Trauner M, Reiberger T, et al. 2019. Detection of various microplastics in human stool: a prospective case series. *Ann Intern Med* 171(7):453–457, PMID: 31476765, <https://doi.org/10.7326/M19-0618>.
  67. Blackburn K, Green D. 2022. The potential effects of microplastics on human health: what is known and what is unknown. *Ambio* 51(3):518–530, PMID: 34185251, <https://doi.org/10.1007/s13280-021-01589-9>.
  68. Wright SL, Kelly FJ. 2017. Plastic and human health: a micro issue? *Environ Sci Technol* 51(12):6634–6647, PMID: 28531345, <https://doi.org/10.1021/acs.est.7b00423>.
  69. Ziani K, Ioniță-Mândrican C-B, Mititelu M, Neacșu SM, Negrei C, Moroșan E, et al. 2023. Microplastics: a real global threat for environment and food safety: a state of the art review. *Nutrients* 15(3):617, PMID: 36771324, <https://doi.org/10.3390/nu15030617>.
  70. Fendall LS, Sewell MA. 2009. Contributing to marine pollution by washing your face: microplastics in facial cleansers. *Mar Pollut Bull* 58(8):1225–1228, PMID: 19481226, <https://doi.org/10.1016/j.marpolbul.2009.04.025>.
  71. Han FY, Thurecht KJ, Whittaker AK, Smith MT. 2016. Bioerodible PLGA-based microparticles for producing sustained-release drug formulations and strategies for improving drug loading. *Front Pharmacol* 7:185, PMID: 27445821, <https://doi.org/10.3389/fphar.2016.00185>.
  72. Rochman CM, Kross SM, Armstrong JB, Bogan MT, Darling ES, Green SJ, et al. 2015. Scientific evidence supports a ban on microbeads. *Environ Sci Technol* 49(18):10759–10761, PMID: 26334581, <https://doi.org/10.1021/acs.est.5b03909>.
  73. Senathirajah K, Attwood S, Bhagwat G, Carbery M, Wilson S, Palanisami T. 2021. Estimation of the mass of microplastics ingested - a pivotal first step towards human health risk assessment. *J Hazard Mater* 404(pt B):124004, PMID: 33130380, <https://doi.org/10.1016/j.jhazmat.2020.124004>.
  74. Scieszka D, Hunter R, Begay J, Bitsui M, Lin Y, Galewsky J, et al. 2022. Neuroinflammatory and neurometabolic consequences from inhaled wildfire smoke-derived particulate matter in the Western United States. *Toxicol Sci* 186(1):149–162, PMID: 34865172, <https://doi.org/10.1093/toxsci/kfab147>.
  75. Wei R, Wang J, Su M, Jia E, Chen S, Chen T, et al. 2018. Missing value imputation approach for mass spectrometry-based metabolomics data. *Sci Rep* 8(1):663, PMID: 29330539, <https://doi.org/10.1038/s41598-017-19120-0>.
  76. Griss J, Viteri G, Sidiropoulos K, Nguyen V, Fabregat A, Hermjakob H. 2020. ReactomeGSA - efficient multi-omics comparative pathway analysis. *Mol Cell Proteomics* 19(12):2115–2125, PMID: 32907876, <https://doi.org/10.1074/mcp.TIR120.002155>.
  77. Milacic M, Beavers D, Conley P, Gong C, Gillespie M, Griss J, et al. 2023. The reactome pathway knowledgebase 2024. *Nucleic Acids Res* 52(D1):D672–D678, <https://doi.org/10.1093/nar/gkad1025>.
  78. Barnes DK, Galgani F, Thompson RC, Barlaz M. 2009. Accumulation and fragmentation of plastic debris in global environments. *Philos Trans R Soc Lond B Biol Sci* 364(1526):1985–1998, PMID: 19528051, <https://doi.org/10.1098/rstb.2008.0205>.
  79. Auta HS, Emenike CU, Fauziah SH. 2017. Distribution and importance of microplastics in the marine environment: a review of the sources, fate, effects, and potential solutions. *Environ Int* 102:165–176, PMID: 28284818, <https://doi.org/10.1016/j.envint.2017.02.013>.
  80. Setälä O, Fleming-Lehtinen V, Lehtiniemi M. 2014. Ingestion and transfer of microplastics in the planktonic food web. *Environ Pollut* 185:77–83, PMID: 24220023, <https://doi.org/10.1016/j.envpol.2013.10.013>.
  81. Huerta Lwanga E, Mendoza Vega J, Ku Quej V, Chi JDLA, Sanchez Del Cid L, Chi C, et al. 2017. Field evidence for transfer of plastic debris along a terrestrial food chain. *Sci Rep* 7(1):14071, PMID: 29074893, <https://doi.org/10.1038/s41598-017-14588-2>.
  82. Kosuth M, Mason SA, Wattenberg EV. 2018. Anthropogenic contamination of tap water, beer, and sea salt. *PLoS One* 13(4):e0194970, PMID: 29641556, <https://doi.org/10.1371/journal.pone.0194970>.
  83. Liebezeit G, Liebezeit E. 2014. Synthetic particles as contaminants in German beers. *Food Addit Contam Part A Chem Anal Control Expo Risk Assess* 31(9):1574–1578, PMID: 25056358, <https://doi.org/10.1080/19440049.2014.945099>.
  84. Möller W, Häussinger K, Winkler-Heil R, Stahlhofen W, Meyer T, Hofmann W, et al. 2004. Mucociliary and long-term particle clearance in the airways of healthy nonsmoker subjects. *J Appl Physiol* (1985) 97(6):2200–2206, PMID: 15347631, <https://doi.org/10.1152/jappphysiol.00970.2003>.

85. Lomer MC, Thompson RP, Powell JJ. 2002. Fine and ultrafine particles of the diet: influence on the mucosal immune response and association with Crohn's disease. *Proc Nutr Soc* 61(1):123–130, PMID: 12002786, <https://doi.org/10.1079/pns2001134>.
86. Beamish LA, Osornio-Vargas AR, Wine E. 2011. Air pollution: an environmental factor contributing to intestinal disease. *J Crohns Colitis* 5(4):279–286, PMID: 21683297, <https://doi.org/10.1016/j.crohns.2011.02.017>.
87. Fournier SB, D'Errico JN, Adler DS, Kollontzi S, Goedken MJ, Fabris L, et al. 2020. Nanopolystyrene translocation and fetal deposition after acute lung exposure during late-stage pregnancy. *Part Fibre Toxicol* 17(1):55, PMID: 33099312, <https://doi.org/10.1186/s12989-020-00385-9>.
88. Sandys O, Te Velde A. 2022. Raising the alarm: environmental factors in the onset and maintenance of chronic (low-grade) inflammation in the gastrointestinal tract. *Dig Dis Sci* 67(9):4355–4368, PMID: 34981314, <https://doi.org/10.1007/s10620-021-07327-1>.
89. Leslie HA, van Velzen MJM, Brandsma SH, Vethaak AD, Garcia-Vallejo JJ, Lamoree MH. 2022. Discovery and quantification of plastic particle pollution in human blood. *Environ Int* 163:107199, PMID: 35367073, <https://doi.org/10.1016/j.envint.2022.107199>.
90. Jenner LC, Rotchell JM, Bennett RT, Cowen M, Tentzeris V, Sadofsky LR. 2022. Detection of microplastics in human lung tissue using muFTIR spectroscopy. *Sci Total Environ* 831:154907, PMID: 35364151, <https://doi.org/10.1016/j.scitotenv.2022.154907>.
91. Munkholm P, Langholz E, Hollander D, Thornberg K, Orholm M, Katz KD, et al. 1994. Intestinal permeability in patients with Crohn's disease and ulcerative colitis and their first degree relatives. *Gut* 35(1):68–72, PMID: 8307453, <https://doi.org/10.1136/gut.35.1.68>.
92. Büning C, Geissler N, Prager M, Sturm A, Baumgart DC, Büttner J, et al. 2012. Increased small intestinal permeability in ulcerative colitis: rather genetic than environmental and a risk factor for extensive disease? *Inflamm Bowel Dis* 18(10):1932–1939, PMID: 22344959, <https://doi.org/10.1002/ibd.22909>.
93. Turpin W, Lee S-H, Raygoza Garay JA, Madsen KL, Meddings JB, Bedrani L, et al. 2020. Increased intestinal permeability is associated with later development of Crohn's disease. *Gastroenterology* 159(6):2092–2100, PMID: 32791132, <https://doi.org/10.1053/j.gastro.2020.08.005>.
94. Teshima CW, Dieleman LA, Meddings JB. 2012. Abnormal intestinal permeability in Crohn's disease pathogenesis. *Ann NY Acad Sci* 1258:159–165, PMID: 22731729, <https://doi.org/10.1111/j.1749-6632.2012.06612.x>.
95. Visser J, Rozing J, Sapone A, Lammers K, Fasano A. 2009. Tight junctions, intestinal permeability, and autoimmunity: celiac disease and type 1 diabetes paradigms. *Ann NY Acad Sci* 1165:195–205, PMID: 19538307, <https://doi.org/10.1111/j.1749-6632.2009.04037.x>.
96. Portincasa P, Bonfrate L, Khalil M, Angelis MD, Calabrese FM, D'Amato M, et al. 2021. Intestinal barrier and permeability in health, obesity and NAFLD. *Biomedicines* 10(1):83, PMID: 35052763, <https://doi.org/10.3390/biomedicines10010083>.
97. Wang Q, Wu Y, Zhang W, Shen T, Li H, Wu J, et al. 2022. Lipidomics and transcriptomics insight into impacts of microplastics exposure on hepatic lipid metabolism in mice. *Chemosphere* 308(pt 3):136591, PMID: 36167205, <https://doi.org/10.1016/j.chemosphere.2022.136591>.
98. Shi C, Han X, Guo W, Wu Q, Yang X, Wang Y, et al. 2022. Disturbed gut-liver axis indicating oral exposure to polystyrene microplastic potentially increases the risk of insulin resistance. *Environ Int* 164:107273, PMID: 35526298, <https://doi.org/10.1016/j.envint.2022.107273>.
99. Wu P, Lin S, Cao G, Wu J, Jin H, Wang C, et al. 2022. Absorption, distribution, metabolism, excretion and toxicity of microplastics in the human body and health implications. *J Hazard Mater* 437:129361, PMID: 35749897, <https://doi.org/10.1016/j.jhazmat.2022.129361>.
100. Handzlik MK, Gengatharan JM, Frizzi KE, McGregor GH, Martino C, Rahman G, et al. 2023. Insulin-regulated serine and lipid metabolism drive peripheral neuropathy. *Nature* 614(7946):118–124, PMID: 36697822, <https://doi.org/10.1038/s41586-022-05637-6>.
101. Grohmann U, Mondanelli G, Belladonna ML, Orabona C, Pallotta MT, Iacono A, et al. 2017. Amino-acid sensing and degrading pathways in immune regulation. *Cytokine Growth Factor Rev* 35:37–45, PMID: 28545736, <https://doi.org/10.1016/j.cytogfr.2017.05.004>.
102. Hasegawa T, Iino C, Endo T, Mikami K, Kimura M, Sawada N, et al. 2020. Changed amino acids in NAFLD and liver fibrosis: a large cross-sectional study without influence of insulin resistance. *Nutrients* 12(5):1450, PMID: 32429590, <https://doi.org/10.3390/nu12051450>.
103. Gaggini M, Carli F, Rosso C, Buzzigoli E, Marietti M, Della Latta V, et al. 2018. Altered amino acid concentrations in NAFLD: impact of obesity and insulin resistance. *Hepatology* 67(1):145–158, PMID: 28802074, <https://doi.org/10.1002/hep.29465>.
104. Lamichhane S, Kempainen E, Trošt K, Siljander H, Hyöty H, Ilonen J, et al. 2019. Circulating metabolites in progression to islet autoimmunity and type 1 diabetes. *Diabetologia* 62(12):2287–2297, PMID: 31444528, <https://doi.org/10.1007/s00125-019-04980-0>.
105. Yang ZS, Bai YL, Jin CH, Na J, Zhang R, Gao Y, et al. 2022. Evidence on invasion of blood, adipose tissues, nervous system and reproductive system of mice after a single oral exposure: nanoplastics versus microplastics. *Biomed Environ Sci* 35(11):1025–1037, PMID: 36443255, <https://doi.org/10.3967/bes2022.131>.
106. Yang Q, Dai H, Cheng Y, Wang B, Xu J, Zhang Y, et al. 2023. Oral feeding of nanoplastics affects brain function of mice by inducing macrophage IL-1 signal in the intestine. *Cell Rep* 42(4):112346, PMID: 37022934, <https://doi.org/10.1016/j.celrep.2023.112346>.
107. Jin H, Yang C, Jiang C, Li L, Pan M, Li D, et al. 2022. Evaluation of neurotoxicity in BALB/c mice following chronic exposure to polystyrene microplastics. *Environ Health Perspect* 130(10):107002, PMID: 36251724, <https://doi.org/10.1289/EHP10255>.
108. Liang B, Huang Y, Zhong Y, Li Z, Ye R, Wang B, et al. 2022. Brain single-nucleus transcriptomics highlights that polystyrene nanoplastics potentially induce Parkinson's disease-like neurodegeneration by causing energy metabolism disorders in mice. *J Hazard Mater* 430:128459, PMID: 35739658, <https://doi.org/10.1016/j.jhazmat.2022.128459>.
109. Yin K, Wang D, Zhao H, Wang Y, Zhang Y, Liu Y, et al. 2022. Polystyrene microplastics up-regulates liver glutamine and glutamate synthesis and promotes autophagy-dependent ferroptosis and apoptosis in the cerebellum through the liver-brain axis. *Environ Pollut* 307:119449, PMID: 35550135, <https://doi.org/10.1016/j.envpol.2022.119449>.
110. Gaspar L, Bartman S, Coppotelli G, Ross JM. 2023. Acute exposure to microplastics induced changes in behavior and inflammation in young and old mice. *Int J Mol Sci* 24(15):12308, PMID: 37569681, <https://doi.org/10.3390/ijms241512308>.
111. Silva-Adaya D, Garza-Lombó C, Gensebatt ME. 2021. Xenobiotic transport and metabolism in the human brain. *NeuroToxicology* 86:125–138, PMID: 34371026, <https://doi.org/10.1016/j.neuro.2021.08.004>.
112. Vethaak AD, Legler J. 2021. Microplastics and human health. *Science* 371(6530):672–674, PMID: 33574197, <https://doi.org/10.1126/science.abe5041>.
113. Prata JC, da Costa JP, Lopes I, Duarte AC, Rocha-Santos T. 2020. Environmental exposure to microplastics: an overview on possible human health effects. *Sci Total Environ* 702:134455, PMID: 31733547, <https://doi.org/10.1016/j.scitotenv.2019.134455>.
114. Chang W-H, Herianto S, Lee C-C, Hung H, Chen H-L. 2021. The effects of phthalate ester exposure on human health: a review. *Sci Total Environ* 786:147371, PMID: 33965815, <https://doi.org/10.1016/j.scitotenv.2021.147371>.
115. Yong CQY, Valiyaveetil S, Tang BL. 2020. Toxicity of microplastics and nanoplastics in mammalian systems. *Int J Environ Res Public Health* 17(5):1509, PMID: 32111046, <https://doi.org/10.3390/ijerph17051509>.
116. Sharma P, Vishwakarma R, Varjani S, Gautam K, Gaur VK, Farooqui A, et al. 2022. Multi-omics approaches for remediation of bisphenol A: toxicity, risk analysis, road blocks and research perspectives. *Environ Res* 215(pt 2):114198, PMID: 36063912, <https://doi.org/10.1016/j.envres.2022.114198>.
117. Barhoumi B, Sander SG, Tolosa I. 2022. A review on per- and polyfluorinated alkyl substances (PFASs) in microplastic and food-contact materials. *Environ Res* 206:112595, PMID: 34929191, <https://doi.org/10.1016/j.envres.2021.112595>.
118. Arrigo F, Impellitteri F, Piccione G, Faggio C. 2023. Phthalates and their effects on human health: focus on erythrocytes and the reproductive system. *Comp Biochem Physiol C Toxicol Pharmacol* 270:109645, PMID: 37149015, <https://doi.org/10.1016/j.cbpc.2023.109645>.
119. Horn DL, Bettcher LF, Navarro SL, Pascua V, Neto FC, Cuschieri J, et al. 2021. Persistent metabolomic alterations characterize chronic critical illness after severe trauma. *J Trauma Acute Care Surg* 90(1):35–45, PMID: 33017357, <https://doi.org/10.1097/TA.0000000000002952>.